Recent Heavy Flavour Results from ATLAS

Marcella Bona

Queen Mary, University of London

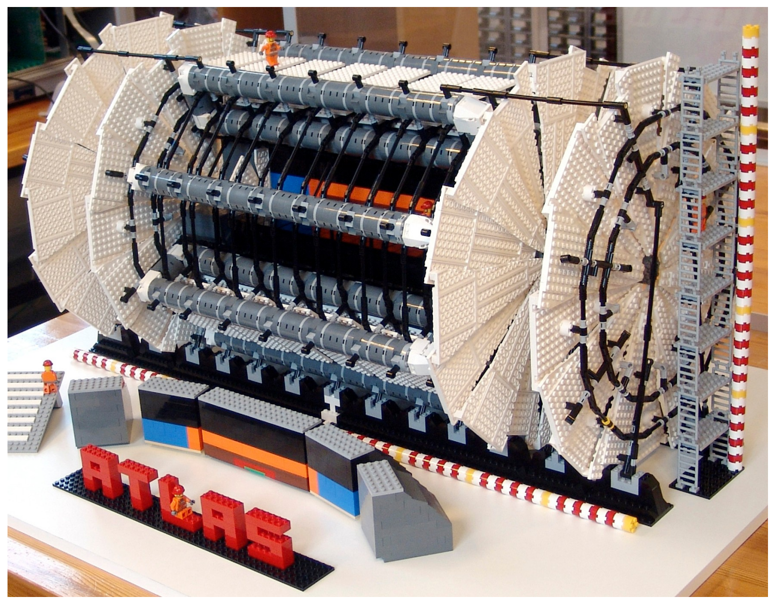

Heavy Ion Collisions in the LHC Era

Quy Nhon, Vietnam

July 18th, 2012

outline

- ATLAS data, detector and triggers
- detector performances
- quarkonia: charmonium and bottomonium
- B meson mass and lifetime measurements
- search for B rare decays: B_s to $\mu\mu$
- $\Delta\Gamma_s$ and ϕ_s measurement from $B_s \to J/\psi\phi$

ATLAS

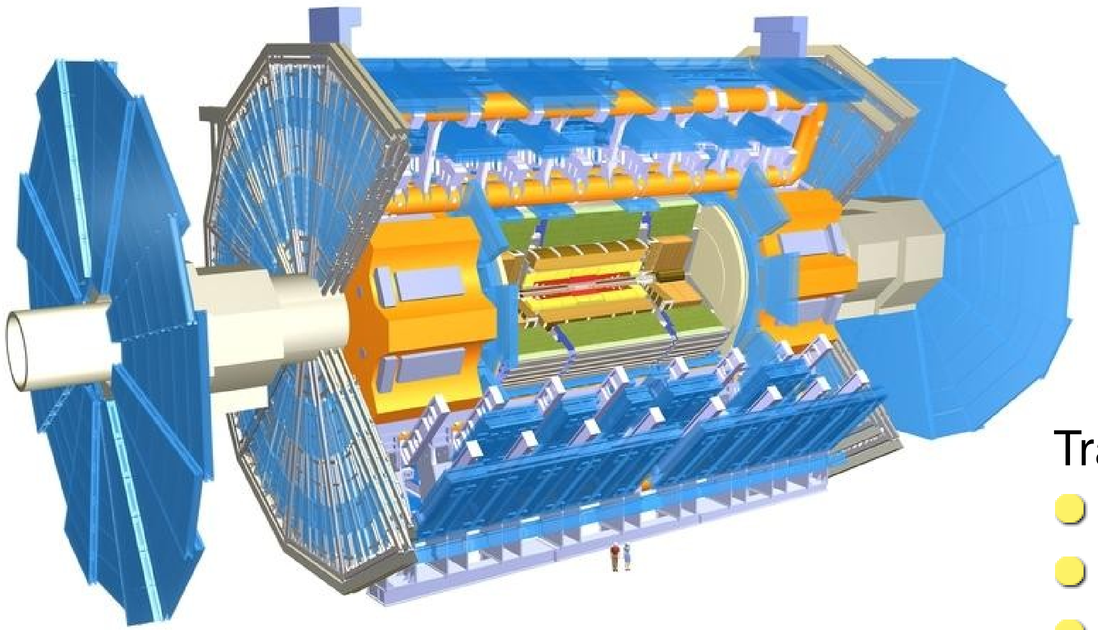

- *Tracking*
  - Silicon (Pixel+Semiconductor tracker) and Transition Radiation Tracker
  - 2T solenoidal field
- *Muon identification:*
  - Dedicated tracking chambers
  - 0.5-2 T toroidal field

Tracking performances:

- 10 μm Impact Parameter resolution
- $\sigma\, p_T/p_T \sim 0.05\%\, p_T \,(+)\, 1.5\%$
- $\sigma\, m(J/\psi\text{-}\Upsilon) \sim 60\text{-}120$ MeV (ID dominated)

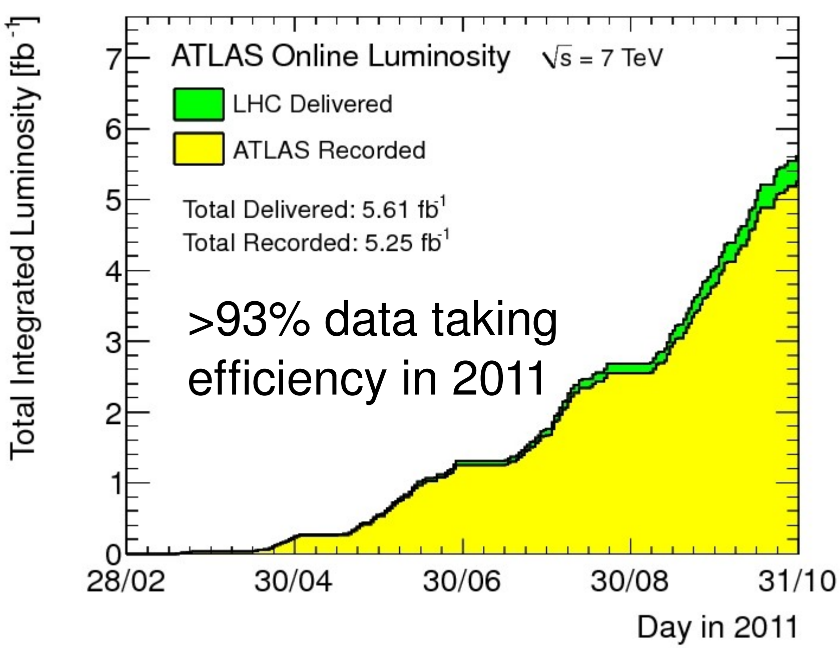

- >5 fb^{-1} recorded in 2011: Instantaneous luminosity and pile-up steadily increasing
- bb-production mostly at large η ATLAS sensitive to $|\eta| < 2.5$ region
  - expect about ~150G B^0–pairs
  - ~30M $B_S \rightarrow J/\psi\phi$ events for 5 fb^{-1}

ATLAS: triggers

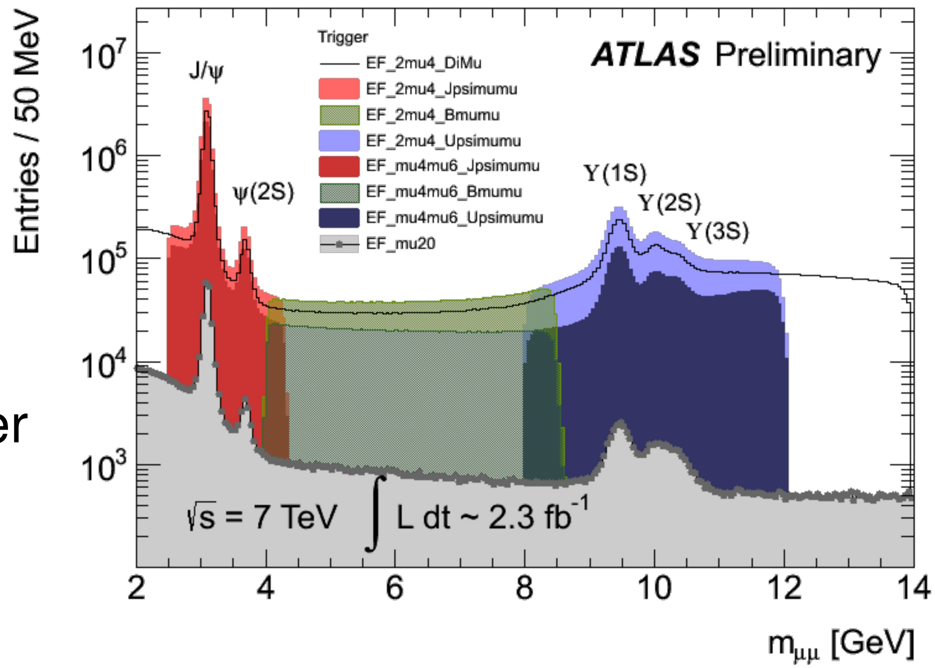

di-muon triggers are our main tool

- As luminosity increases, bandwidth requirements are more stringent
- Potentially forced to higher p_T

Level1 4-GeV muon selections made cleaner

- we ran with constant trigger thresholds for di-muons all across 2011

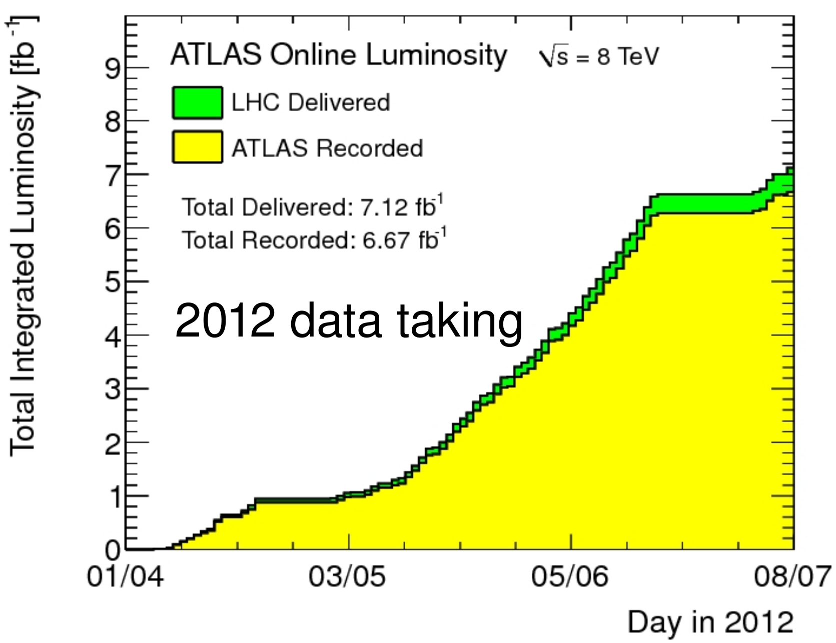

> 6 fb^{-1} of data already collected in 2012

- higher muon p_T thresholds would affect the efficiency for B physics
- specific di-muon selections with Barrel/Endcap logic
- 4 p_T di-muon triggers collected but processed later in time (2013 shutdown)

performances

Nucl. Phys. B, Vol. 850, 387-444 (2011)

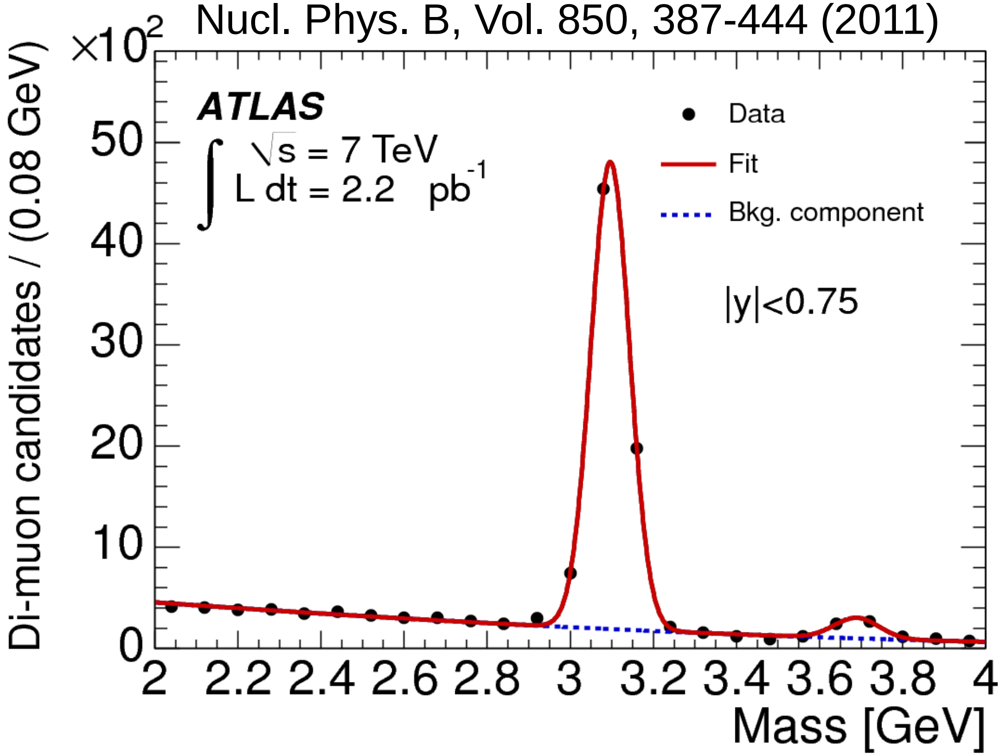

JINST 3 S08003 (2008)

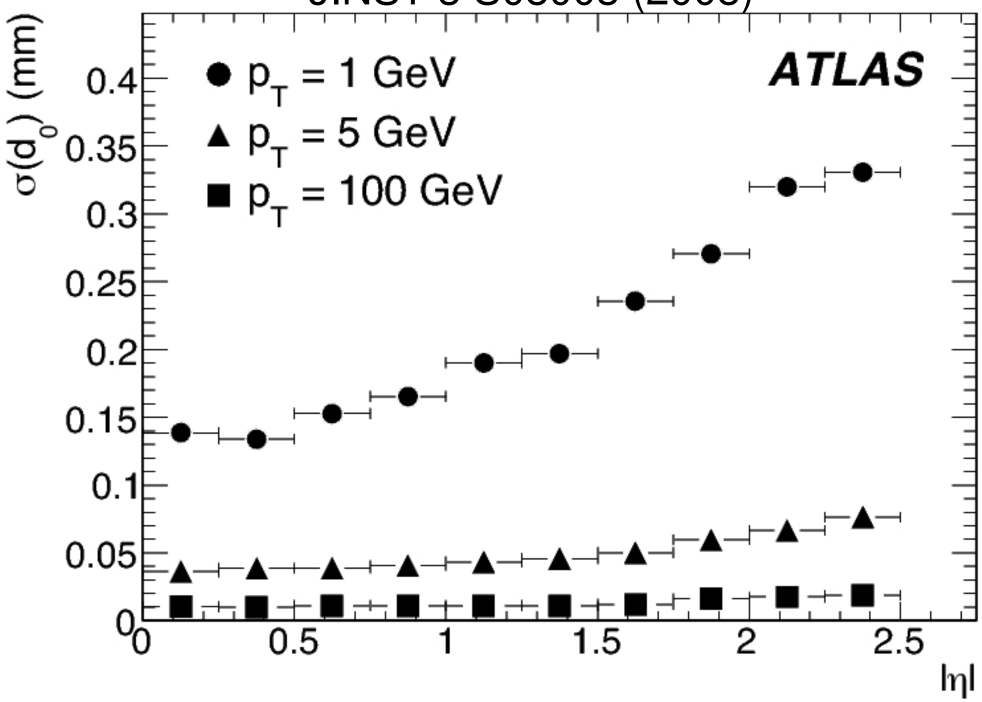

- good mass resolution required for good S/B performance
  - limited particle ID: only for $p_T < 1$GeV/c K/π separation possible
- good impact parameter resolution required for lifetime measurements

tracking-vertexing performance in pile-up

- Vertex resolution important for precision B-physics measurements: lifetime, CPV, rare decays.

- Quality of vertexing monitored over 2011 as pileup increased

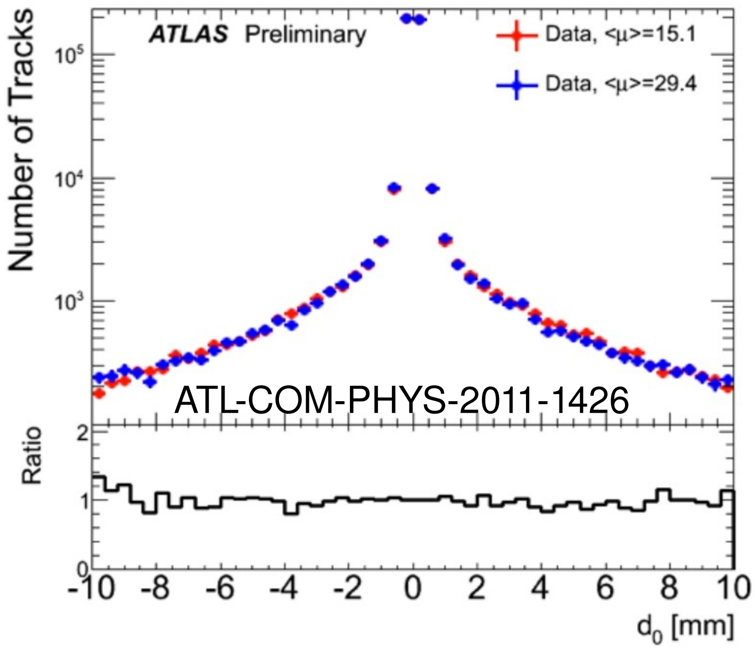

- d_0 (top plot) of the reconstructed tracks with respect to the PV for 2 different number of pileups:
  - The tails are sensitive to the rate of secondaries and fakes. No significant increase in the fake rate observed.

- Good z-resolution of primary vertex (bottom plot) important at high luminosities

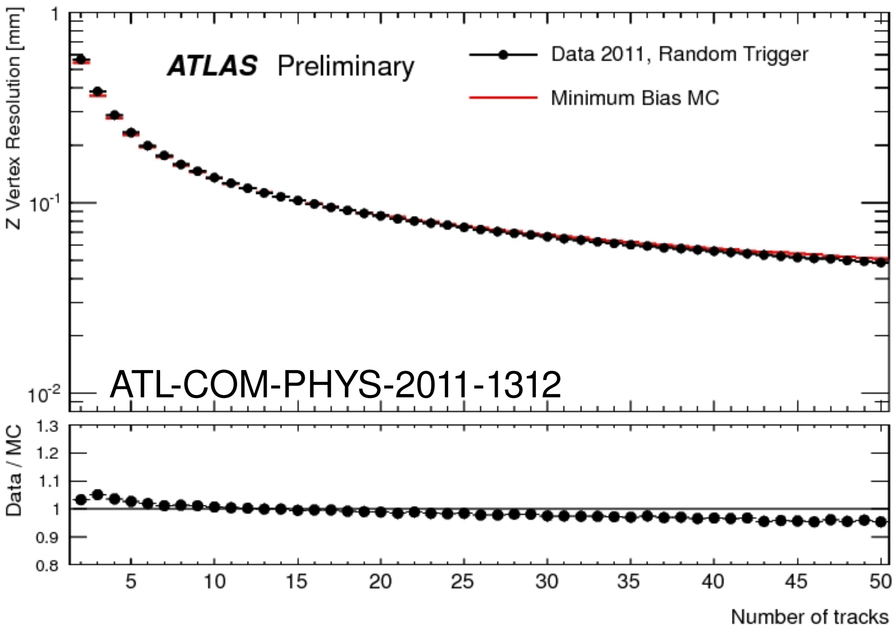

measurement of the centrality dependence of J/ψ yields

- very first results on 6.7 μb^{-1} 2010 data

Phys. Lett. B 697 (2011) 294–312

- minimum-bias trigger, centrality percentiles defined from the total transverse energy, $\sum E_T^{FCal}$, measured in the forward calorimeter (Fcal), covering $3.2 < |\eta| < 4.9$.

$$N_c^{corr}(J/\psi \to \mu^+\mu^-) = \frac{N^{meas}(J/\psi \to \mu^+\mu^-)_c}{\epsilon(J/\psi)_c \cdot W_c}$$

- centrality-dependent suppression observed in J/ψ mesons produced in the collisions of lead ions

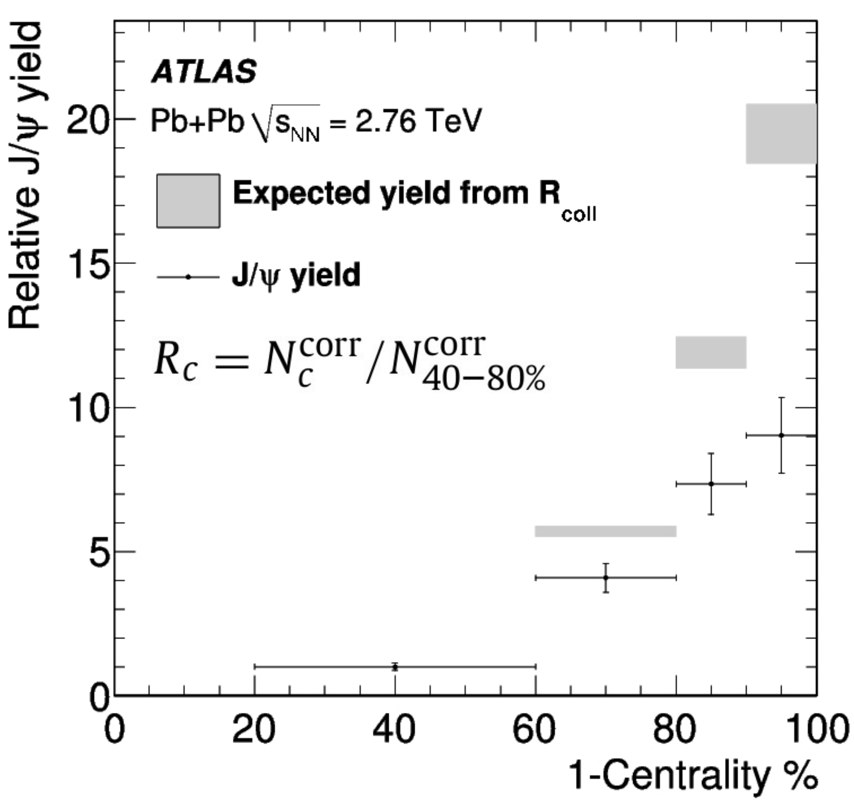

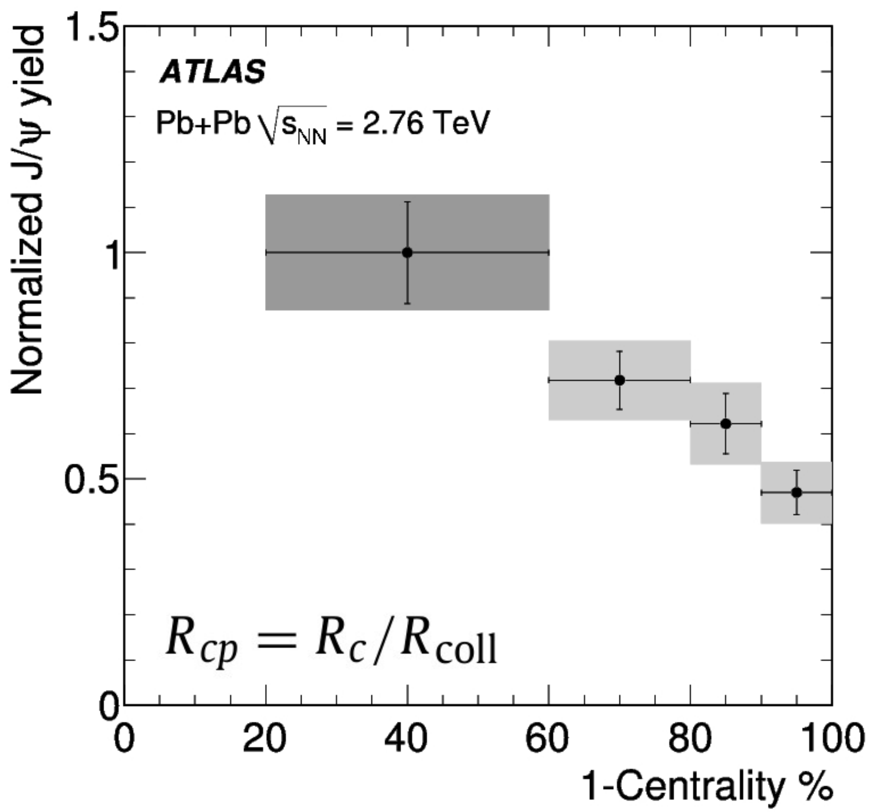

heavy quarkonium physics

- Charmonia (cc) and bottomonia (bb) provide a good testing ground for p-QCD studies
- Production not well understood, Color Singlet (CS) and Color Octet (CO) mechanisms describe p_T spectrum observed at Tevatron but polarization predictions disagree with measurements

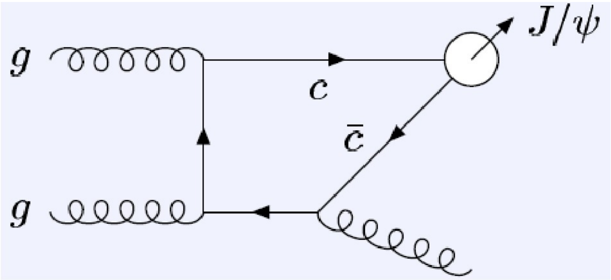

Color singlet (CS) LO diagram

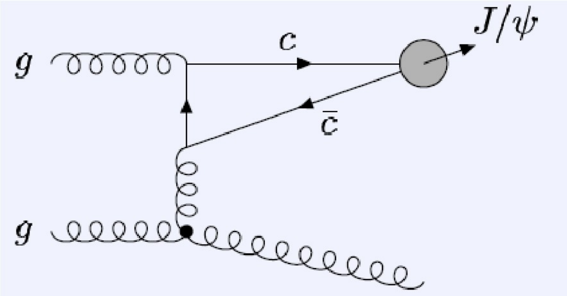

Color octet (CO) LO diagram

- Onia production occurs through:
  - Prompt production:
    - Direct production,
    - Feed-down from higher quarkonium states.
  - Non-prompt production:
    - From decays of B hadrons (only charmonium).

- Experimental hadron spectroscopy has an essential role in understanding of the QCD, LHC allows reaching higher p_T and rapidity regions.

charmonium

- Bound state of $c\bar{c}$ with many excited states
  - J/ψ and its radial excitation ψ(2S) are easily observed with the detector
  - BR(J/ψ → μμ) ~ 5.97 %
  - Important for B-meson decays studies

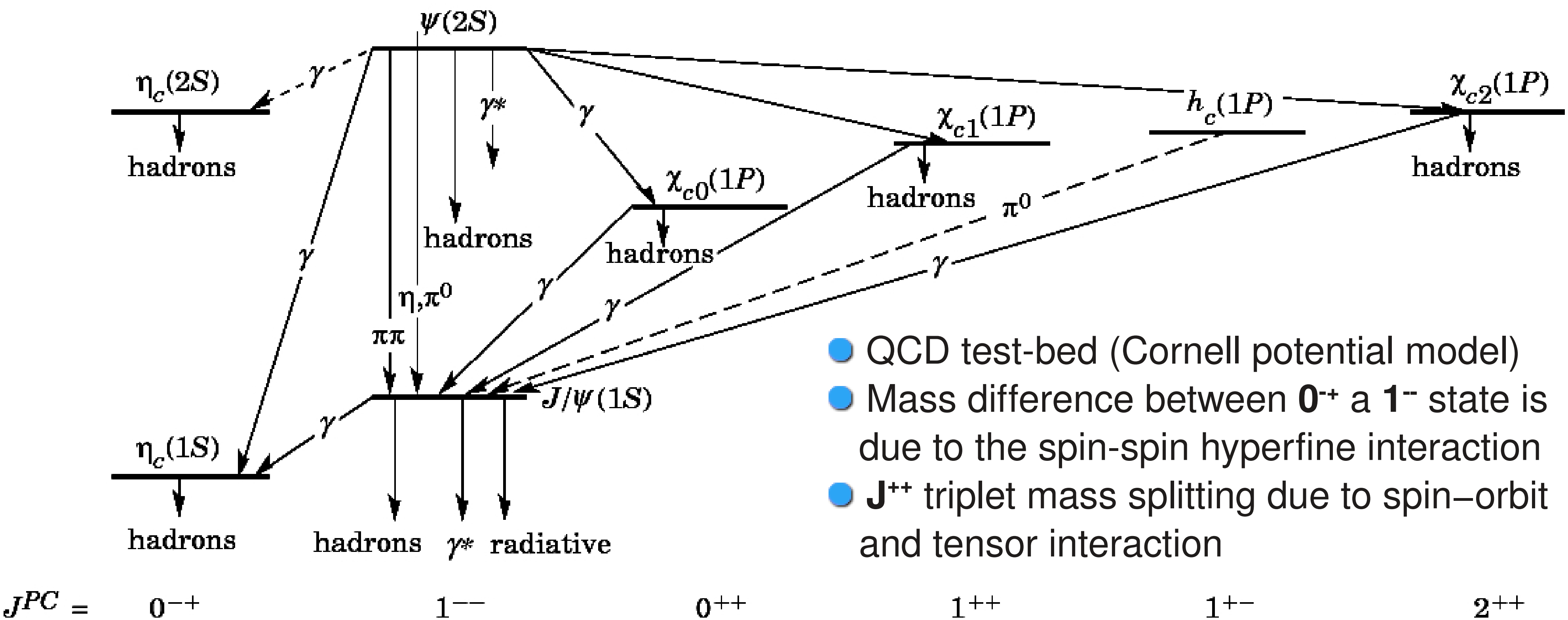

- QCD test-bed (Cornell potential model)
- Mass difference between **0**$^{-+}$ a **1**$^{--}$ state is due to the spin-spin hyperfine interaction
- **J**$^{++}$ triplet mass splitting due to spin–orbit and tensor interaction

J/ψ differential production cross section

- J/ψ candidates identified through di-muon decays:
  experimentally clean; BR ~ 6%

Nucl. Phys. B850, 387-444 (2011)

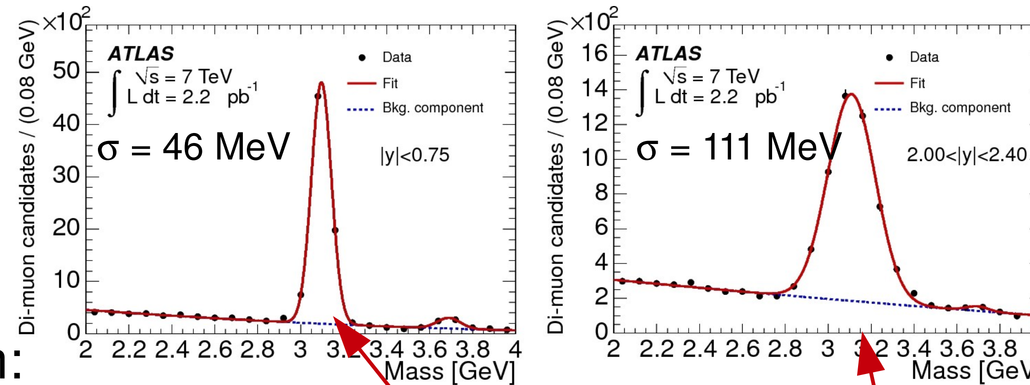

- Separate events into bins of p_T–rapidity for differential analysis

- Per-candidate weights applied to correct for detector inefficiencies from:
  muon reconstruction, trigger efficiencies, and detector acceptance

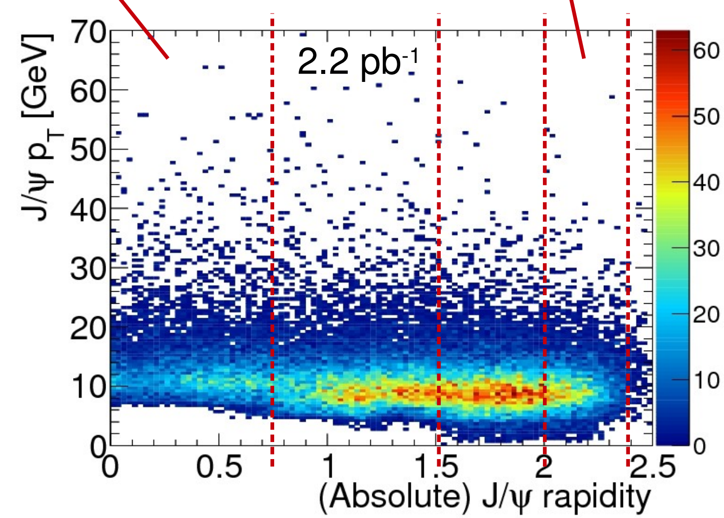

$$w^{-1} = \mathcal{A} \cdot \mathcal{M} \cdot \mathcal{E}^2_{\mathrm{trk}} \cdot \mathcal{E}^+{}_\mu(p_T^+, \eta^+) \cdot \mathcal{E}^-{}_\mu(p_T^-, \eta^-) \cdot \mathcal{E}_{\mathrm{trig}}$$

Detector acceptance ($\mathcal{A}$); **Bin migration** ($\mathcal{M}$); **ID reco efficiency** (per muon track) ($\mathcal{E}^2_{\mathrm{trk}}$); **Reconstruction efficiency** ($\mathcal{E}^\pm{}_\mu$); **Trigger efficiency** ($\mathcal{E}_{\mathrm{trig}}$)

- Binned fit to weighted mass-distributions determines corrected yields in each bin:
  extract differential inclusive cross-section

$$\frac{d^2\sigma(J/\psi)}{dp_T dy} Br(J/\psi \to \mu^+\mu^-) = \frac{N^{J/\psi}_{corr}}{\mathcal{L} \cdot \Delta p_T \Delta y}$$

J/ψ: non-prompt fraction

$$\tau = \frac{L_{xy}\, m(J/\psi)}{p_T(J/\psi)}$$

xy displacement of candidate from PV (L_{xy})
Invariant mass of candidate ($m(J/\psi)$)
p_T of candidate ($p_T(J/\psi)$)

- Discriminate between prompt and non-prompt components from 2-d mass-lifetime fit
  - prompt J/ψ have τ consistent with zero
  - non-prompt J/ψ have τ >0
- Measured τ is convoluted with the detector resolution function

Nucl. Phys. B850, 387-444 (2011)

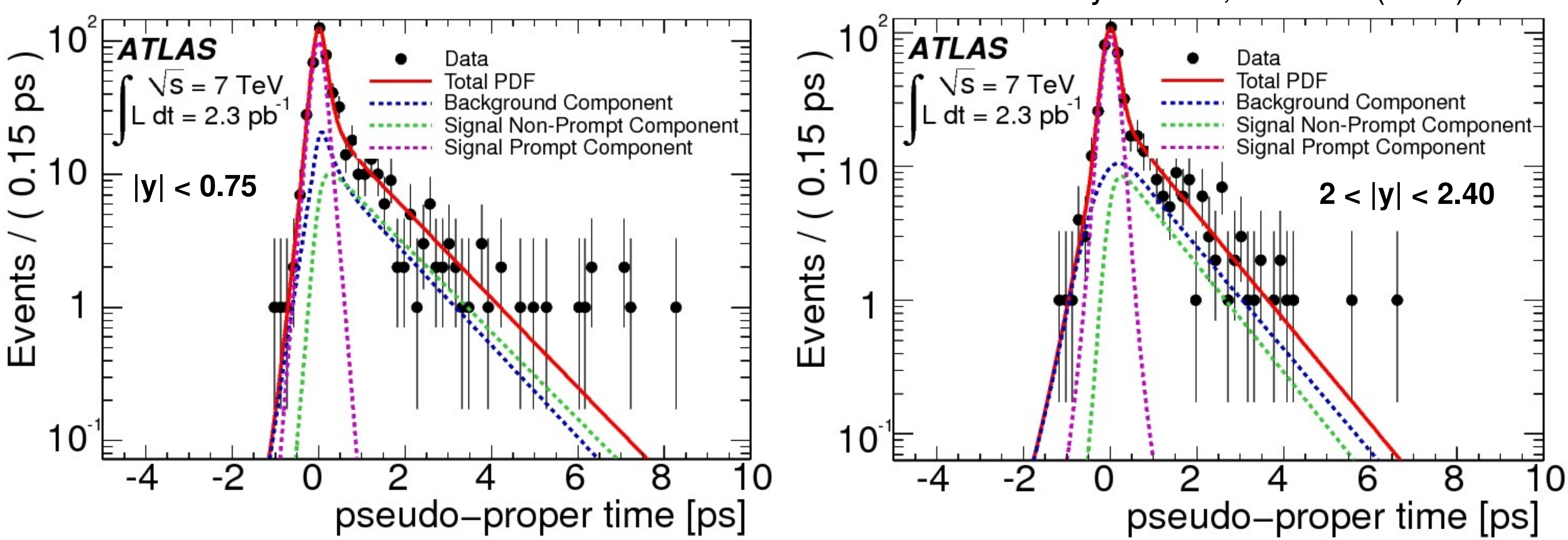

J/ψ: non-prompt fraction

xy displacement of candidate from PV

Invariant mass of candidate

$$\tau = \frac{L_{xy}\, m(J/\psi)}{p_T(J/\psi)}$$

p_T of candidate

- Discriminate between prompt and non-prompt components from 2-d mass-lifetime fit

- Non-prompt J/ψ fraction as a function of momentum for different rapidity regions
- Yellow bands represent polarization uncertainty

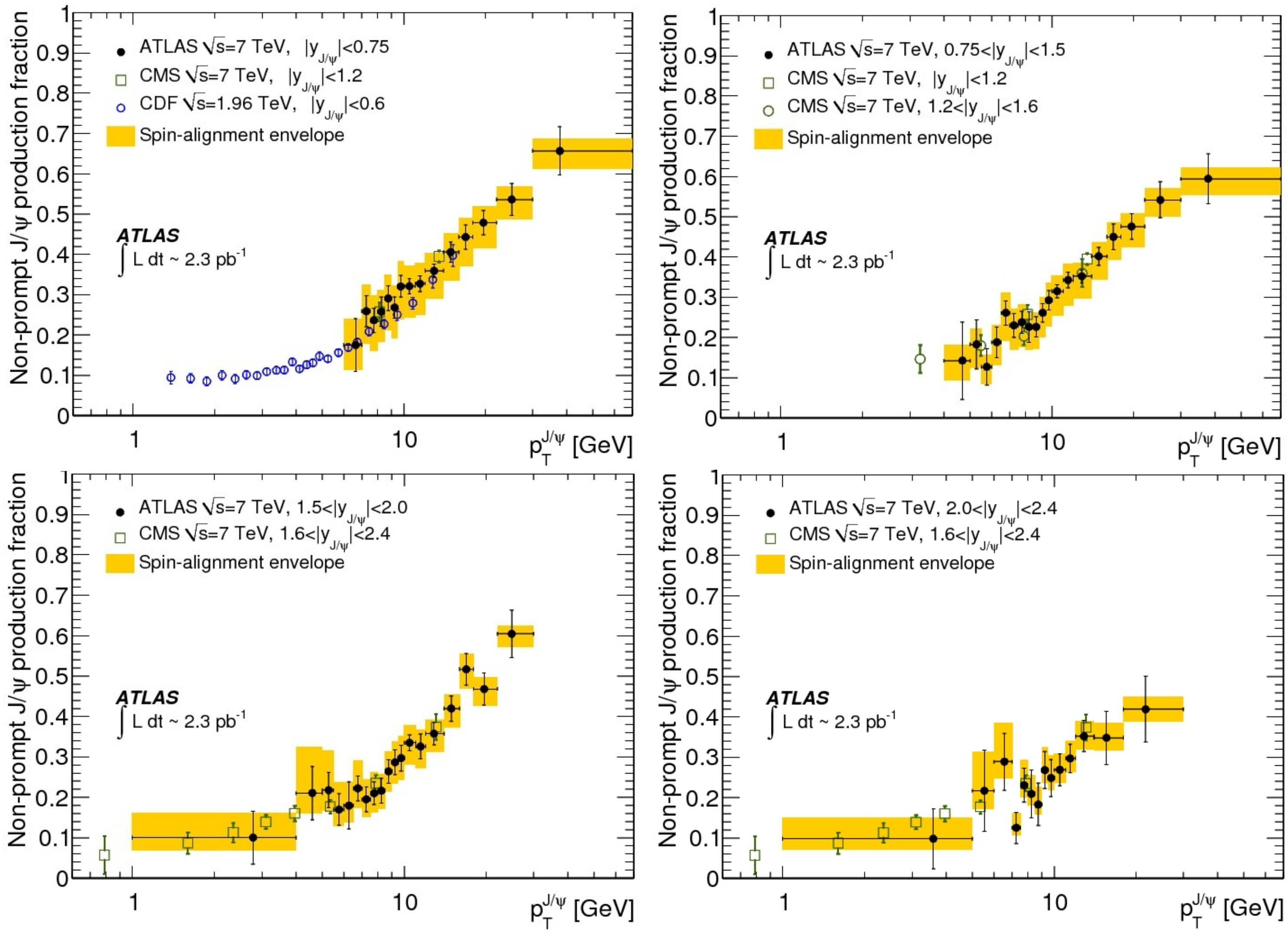

Not updated to newest CMS result, see JHEP02 (2012)011

Nucl. Phys. B850, 387-444 (2011)

J/ψ: non-prompt cross-section

- non-prompt cross-section agrees well with FONLL* predictions

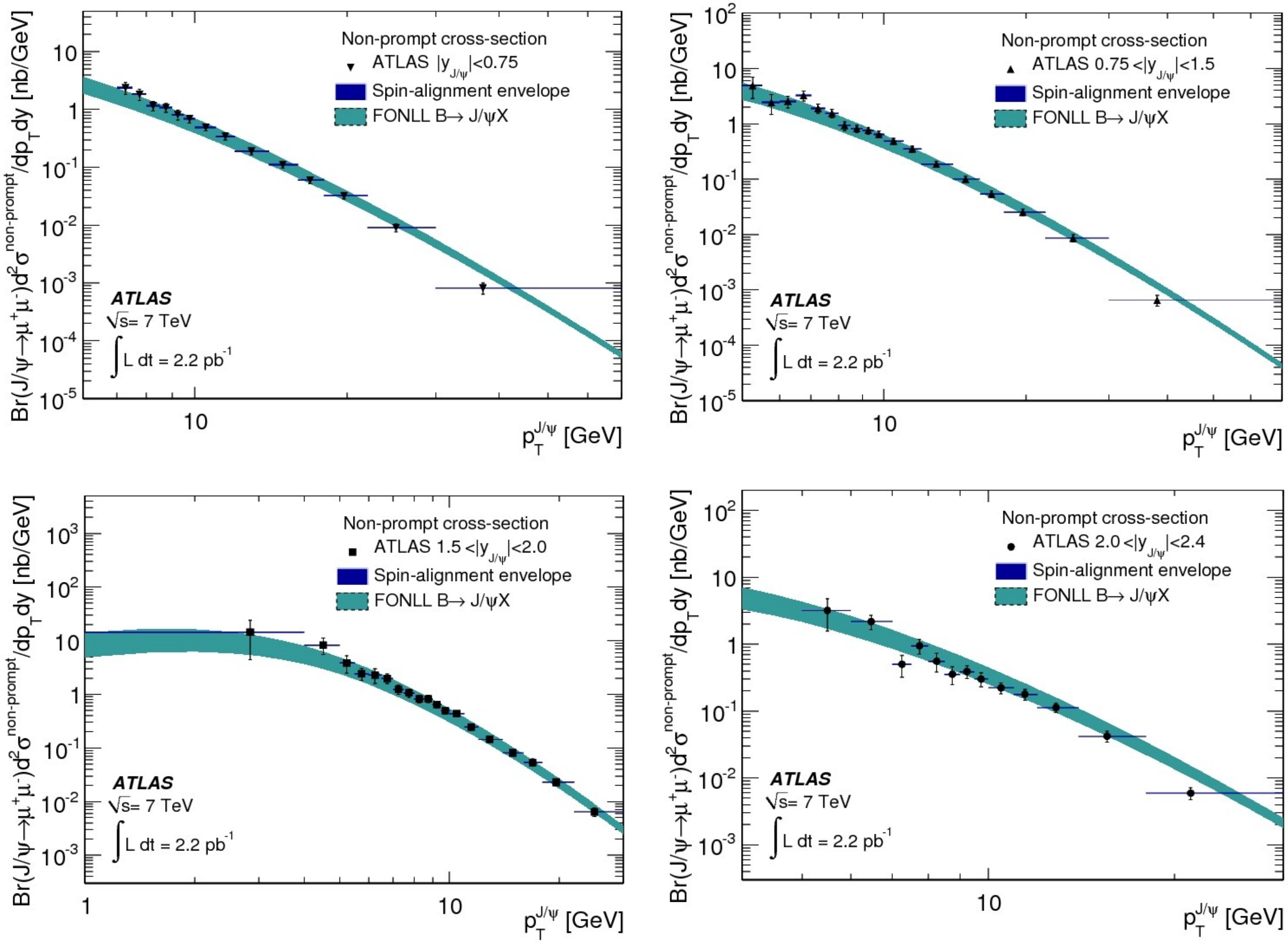

*Fixed-Order Next-to-Leading Log

Nucl. Phys. B850, 387-444 (2011)

J/ψ: prompt cross-section

Color Evaporation model: not a good description of shape

Color Singlet model@NLO: good shape description but underestimating the scale

Color Singlet model@NNLO: significantly better than previous models

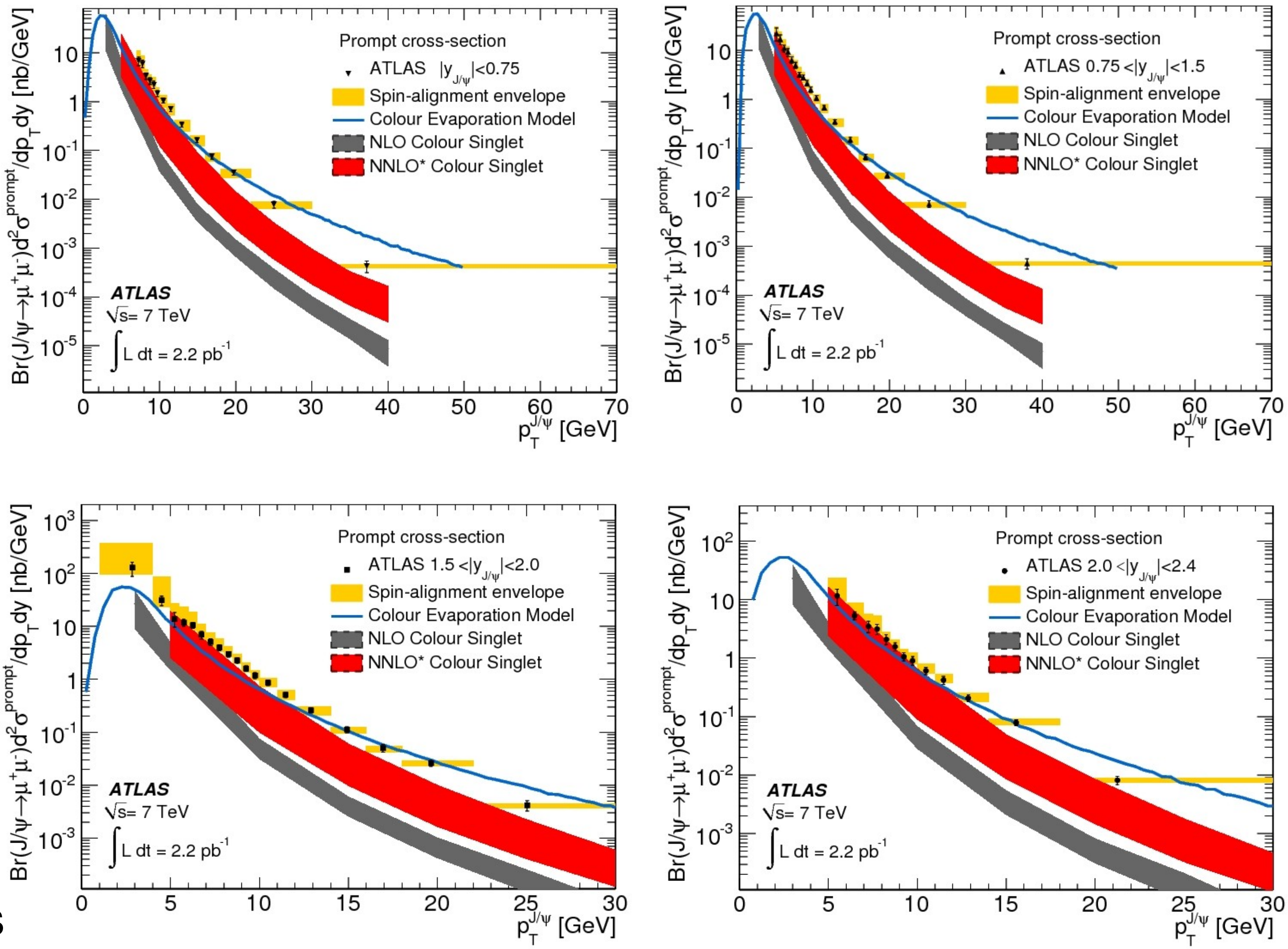

Nucl. Phys. B850, 387-444 (2011)

spectroscopy: observation of χ_{cJ}(1P) state

- Contribution to S-wave charm(bottom)-onium states through feed-down of the P-wave χ_c and χ_b states considerable (~ 1/3)
  - Measurement of these feed-down processes key in overall understanding of quarkonium production

ATLAS-CONF-2011-136

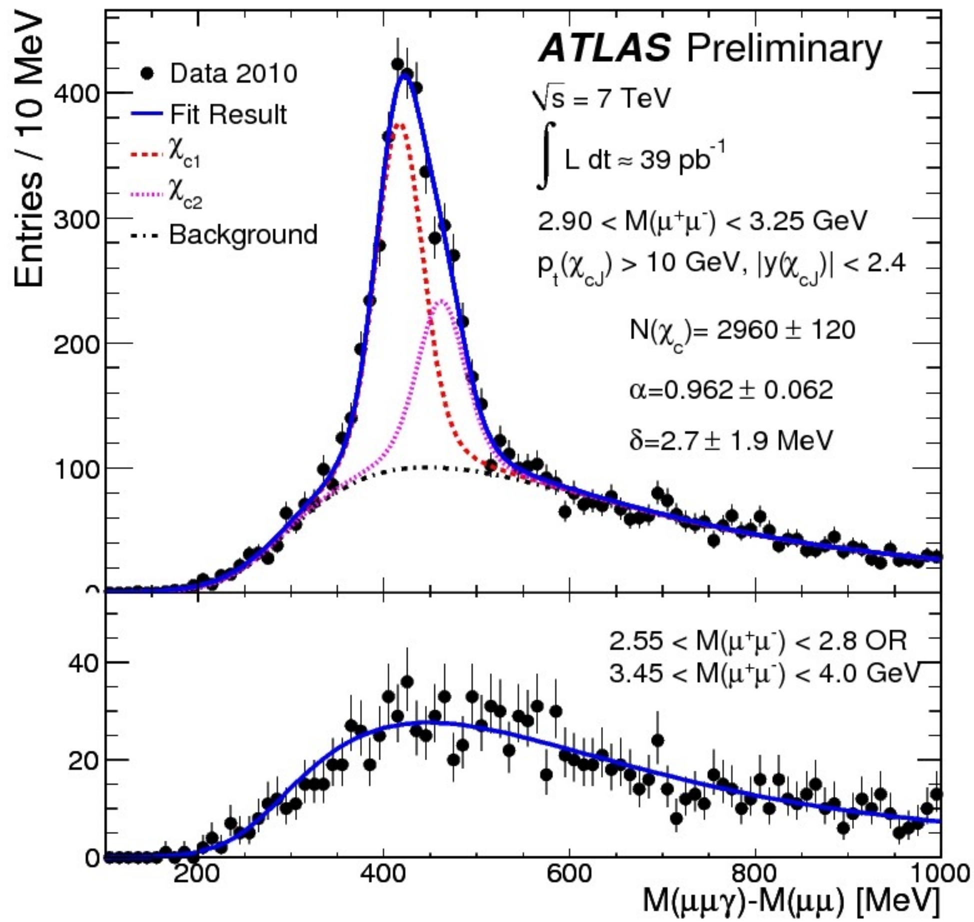

- Experimentally, observe χ_c through its radiative decays to J/ψ:
  - Challenge of reconstructing soft-photon through calorimetry or tracking (via conversions to electron pairs).

- Construct the Mass difference:
  - $\Delta m = m(\mu\mu\gamma) - m(\mu\mu)$
    - Effectively removes contribution of the di-muon resolution.

- χ_c observation using photons identified in electromagnetic calorimeter.
  - Background shape determined from di-muon sideband region.
  - χ_{c0} contribution neglected – small branching fraction through radiative decays.

bottomonium

Bound state of $b\bar{b}$
Richer structure than charmonium
due to higher $\bar{B}B$ threshold
Three states $\Upsilon(1S)$, $\Upsilon(2S)$ and $\Upsilon(3S)$
decay to $\mu\mu$ pairs with BR about 2%

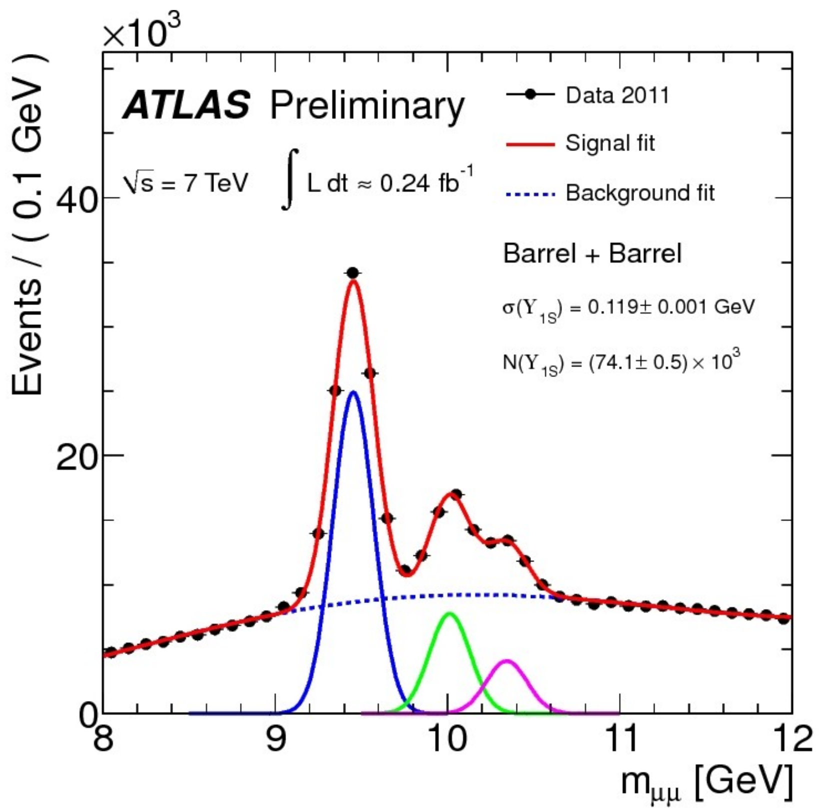

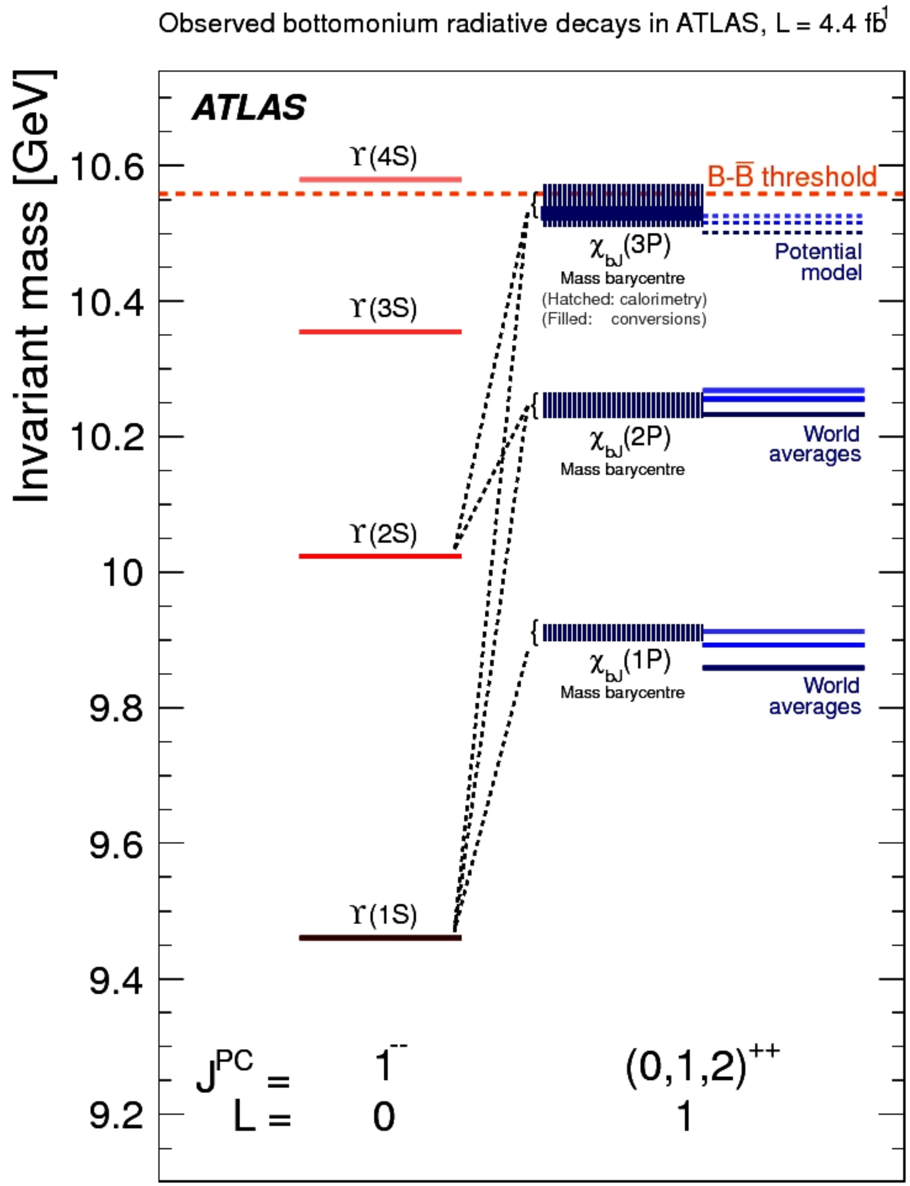

spectroscopy: observation of χ_b system

- Observation of χ_b system similar to χ_c:
  observed through radiative decays to Υ
  Υ identified through di-muon decay

- Data from 2011 at 7 TeV: 4.4 fb^{-1}

- Photons identified through both:
  Calorimetric measurement:
  - High efficiency
  - Threshold reconstruction energy: 2.5 GeV

  Tracking-based through conversions
  ($\gamma \rightarrow e^+e^-$ in silicon of the inner detector)
  - Small probability(conversion) x reco. eff.
  - Lower threshold p_T >1 GeV

  Photons not compatible with originating from di-muon vertex rejected.

Phys. Rev. Lett. 108 (2012) 152001

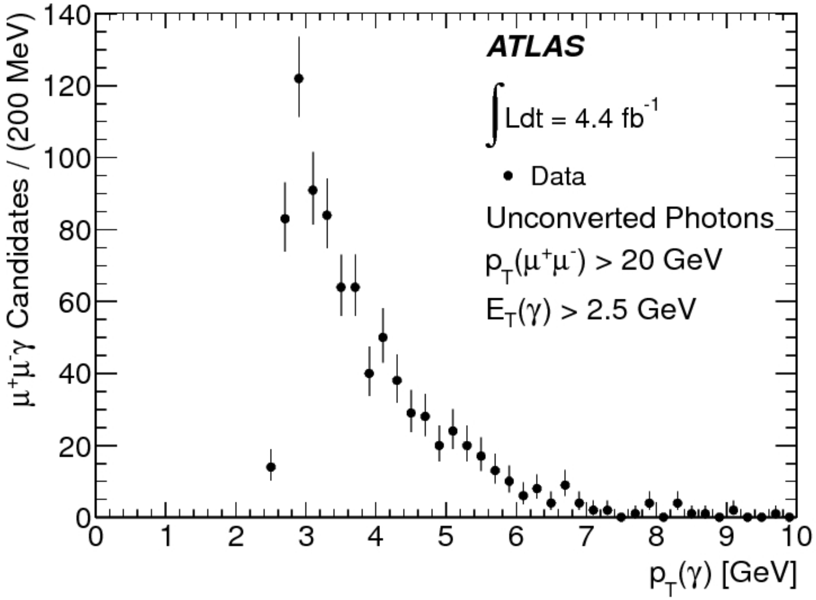

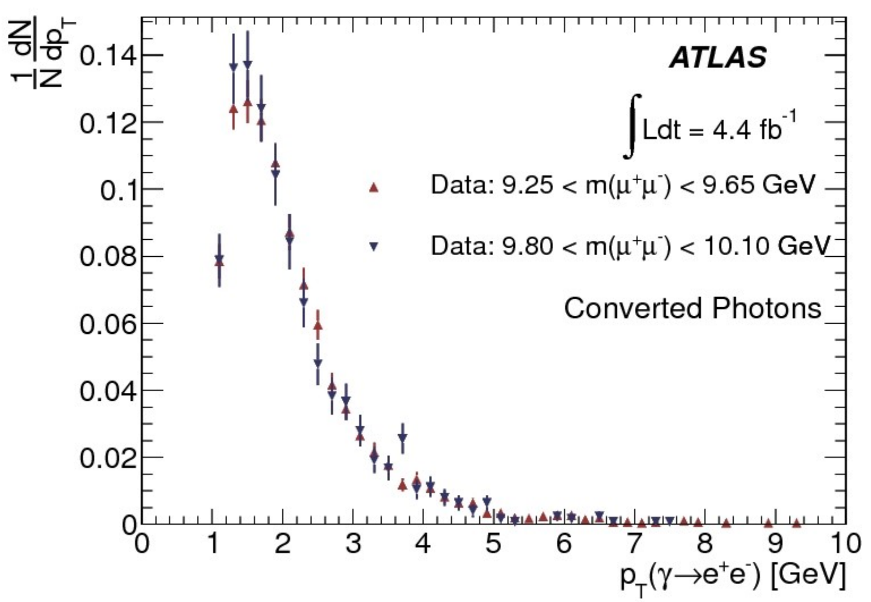

observation of $\chi_b(3P)$ state

- New triplet states observed
  via radiative decays $\chi_{bJ} \rightarrow \Upsilon(1S,2S)\ \gamma$

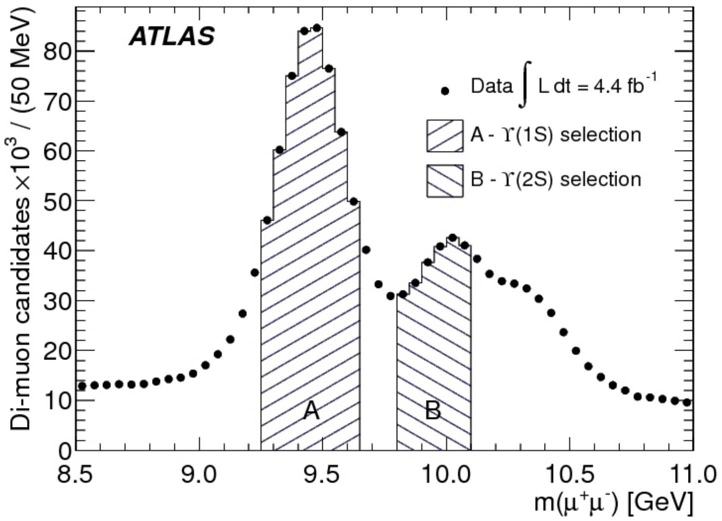

Phys. Rev. Lett. 108 (2012) 152001

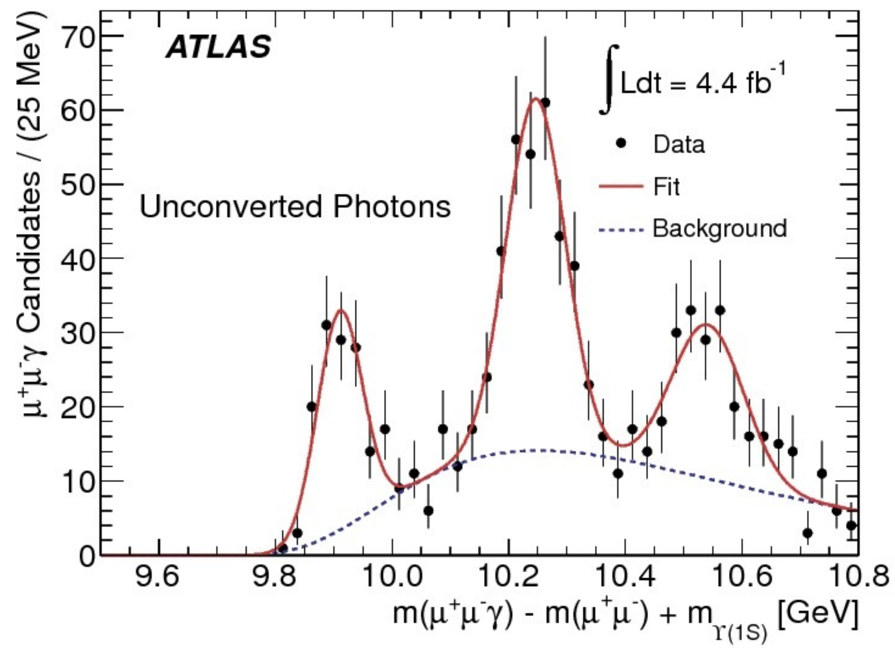

- Plot $\Delta m + m(\Upsilon)$ distribution:
  $\chi_b(1P)$ and $\chi_b(2P)$ observed.
  First observation of new χ_b state.
  Interpreted as $\chi_b(3P)$.

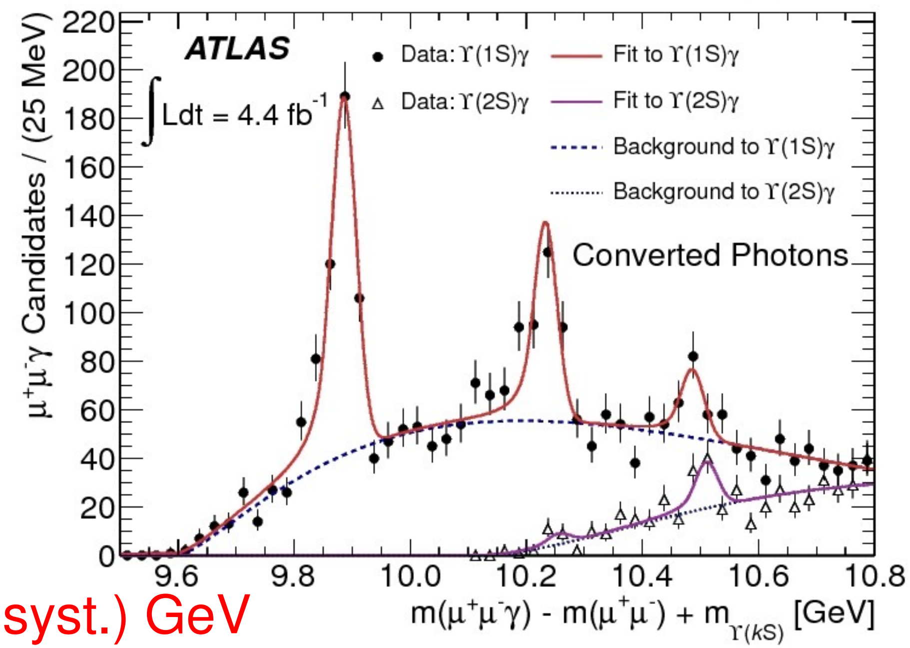

- Using converted photons:
  $m(\chi_b(3P)) = 10.53 \pm 0.005\ (stat.) \pm 0.009\ (syst.)$ GeV
  consistent with predictions

DØ confirms a similar signal: see FERMILAB-PUB-12-084-E

B-hadrons mass signals, updates 2011

- in the first data (2010-2011) masses of all B-hadrons measured in exclusive decays with $J/\psi(\mu\mu)$
- Consistency with PDG - showed that p_T scale well understood also down to low p_T values
- Latest updates using 2011 data shown here for Λ_b and B_c

The solid line is the projection of the results of the unbinned maximum likelihood fits

ATLAS-CONF-2011-105

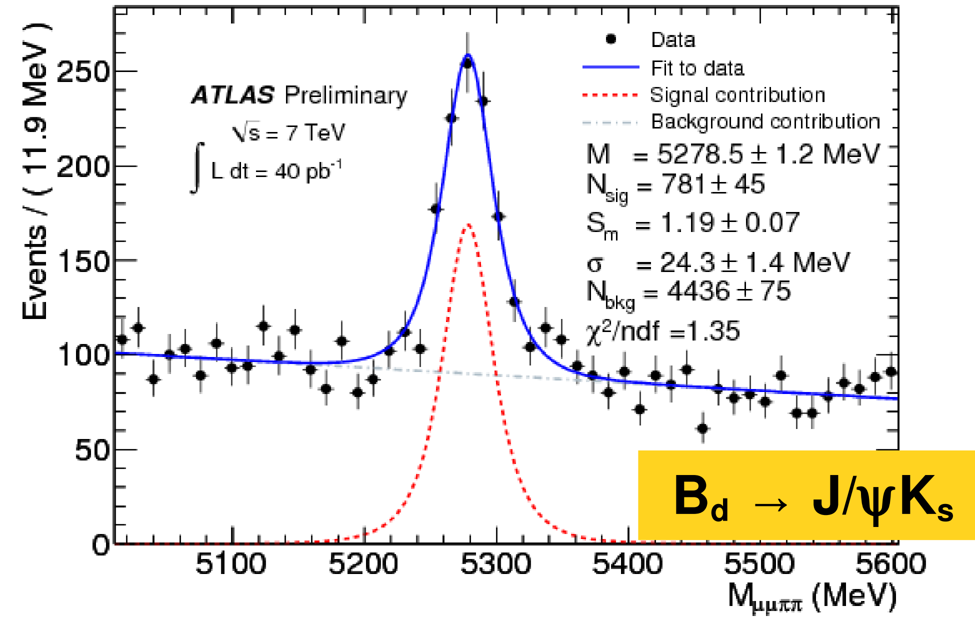

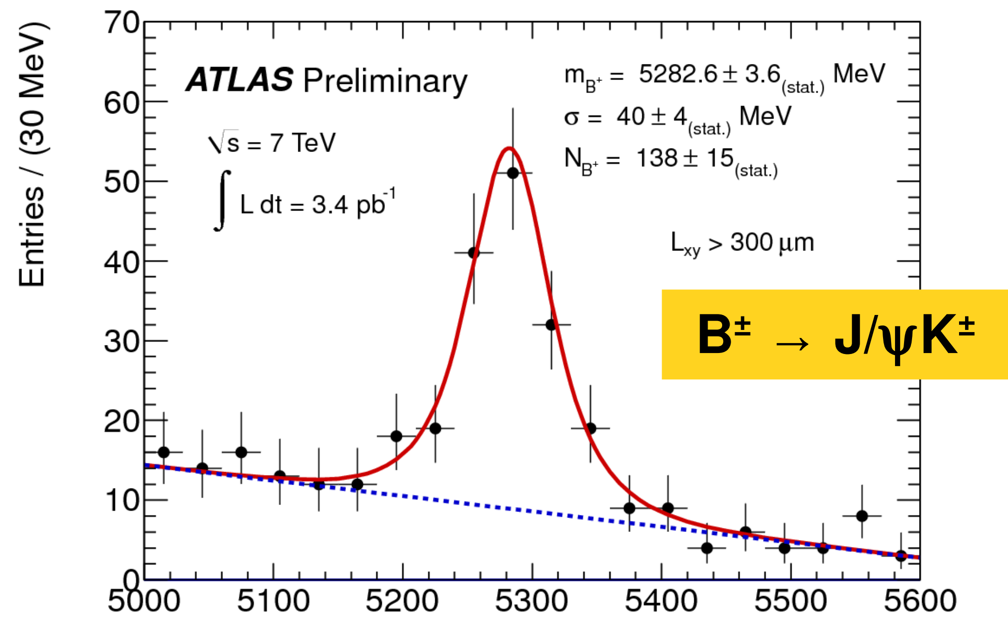

ATLAS-CONF-2010-098

B-hadrons mass signals, updates 2011

- in the first data (2010-2011) masses of all B-hadrons measured in exclusive decays with $J/\psi(\mu\mu)$

- Consistency with PDG - showed that p_T scale well understood also down to low p_T values

- Latest updates using 2011 data shown here for Λ_b and B_c

The solid line is the projection of the results of the unbinned maximum likelihood fits

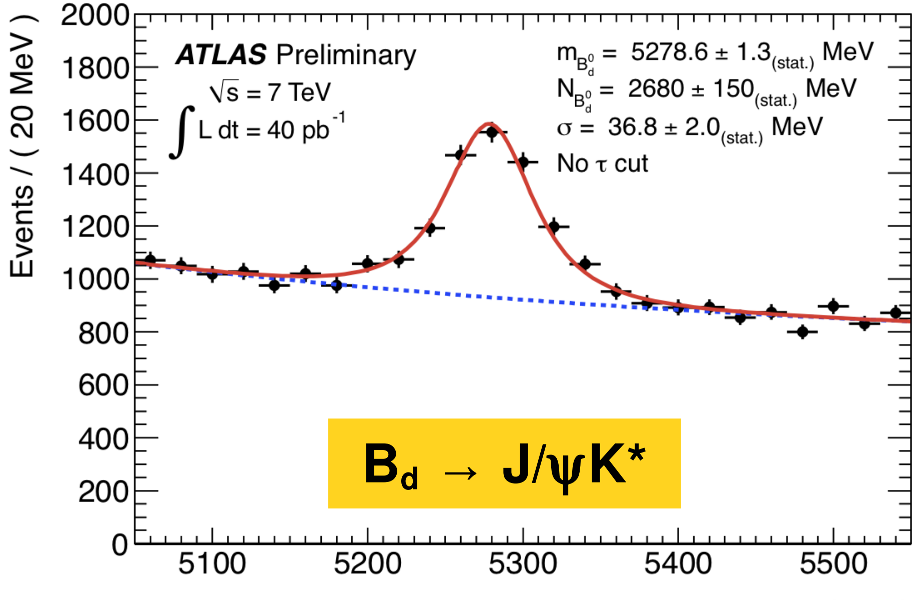

ATLAS-CONF-2011-050

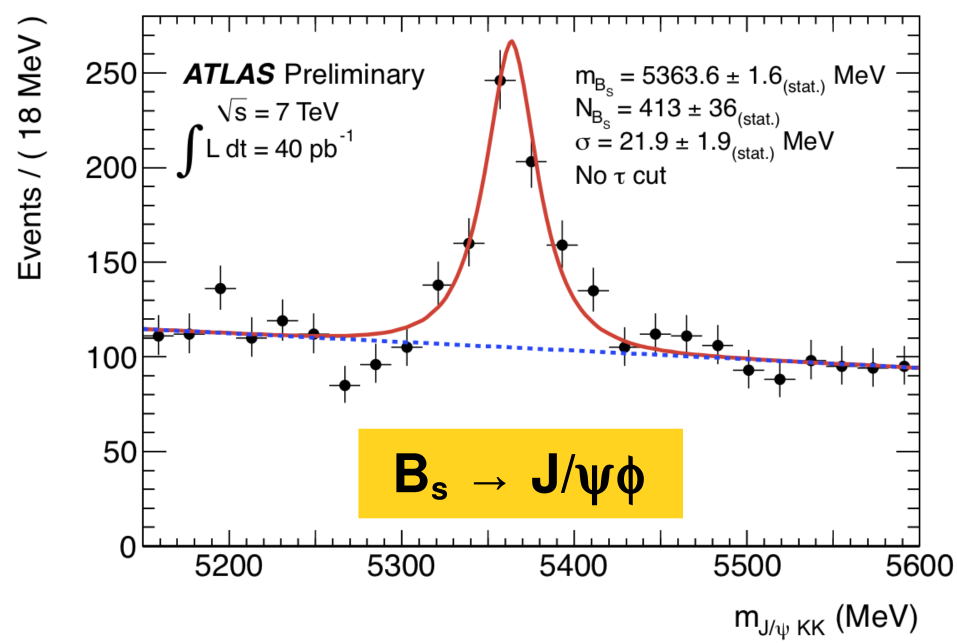

B-hadrons mass signals, updates 2011

- in the first data (2010-2011) masses of all B-hadrons measured in exclusive decays with $J/\psi(\mu\mu)$
- Consistency with PDG - showed that p_T scale well understood also down to low p_T values
- Latest updates using 2011 data shown here for Λ_b and B_c

The solid line is the projection of the results of the unbinned maximum likelihood fits

ATLAS-CONF-2011-124

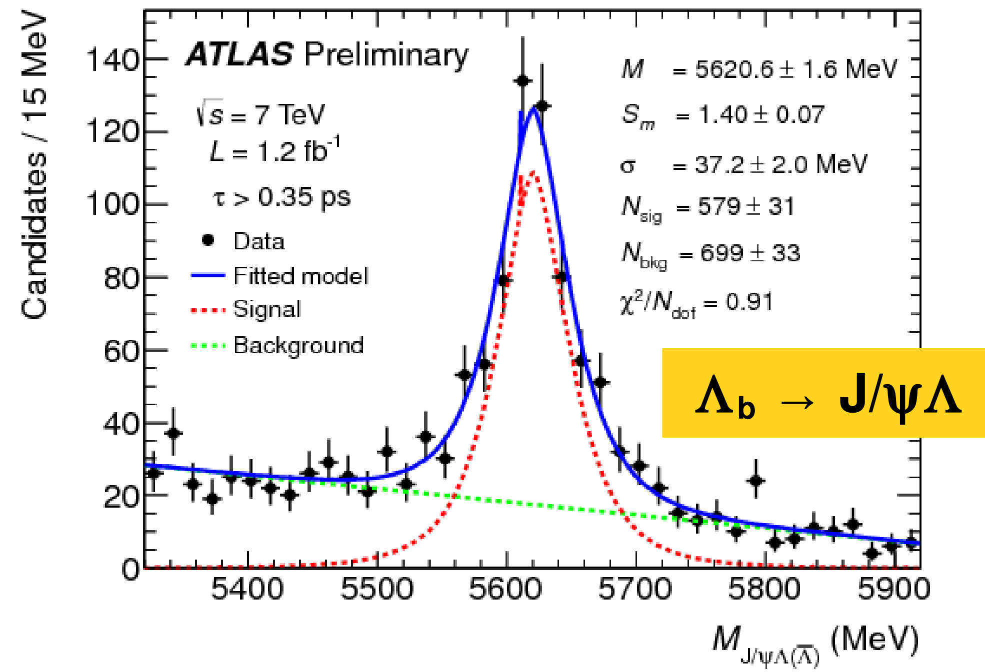

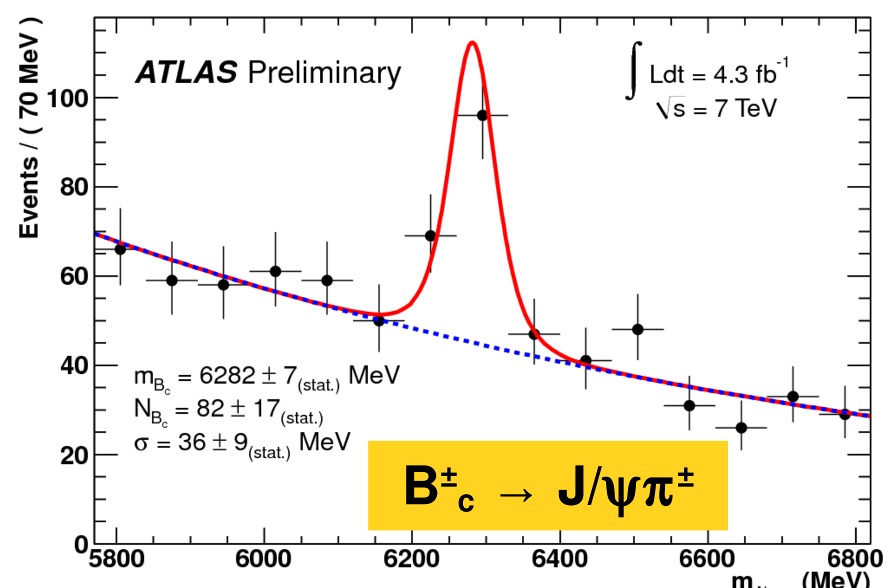

ATLAS-CONF-2012-028

ATLAS-CONF-2012-055

Λ_b mass and lifetime

- update to total 2011 data: 4.9 fb^{-1}
- $\Lambda_b^0 \to J/\psi\ (\mu\mu)\ \Lambda^0\ (p^+\pi^-)$
- background from prompt and non-prompt J/y
- simultaneous unbinned maximum likelihood fit to mass and lifetime
- mass result competitive with the world average

$$\tau = \frac{L_{xy} m^{\mathrm{PDG}}}{p_{\mathrm{T}}}$$

$$m_{\Lambda_b} = 5619.7 \pm 0.7(\mathrm{stat}) \pm 1.1(\mathrm{syst})\ \mathrm{MeV}$$

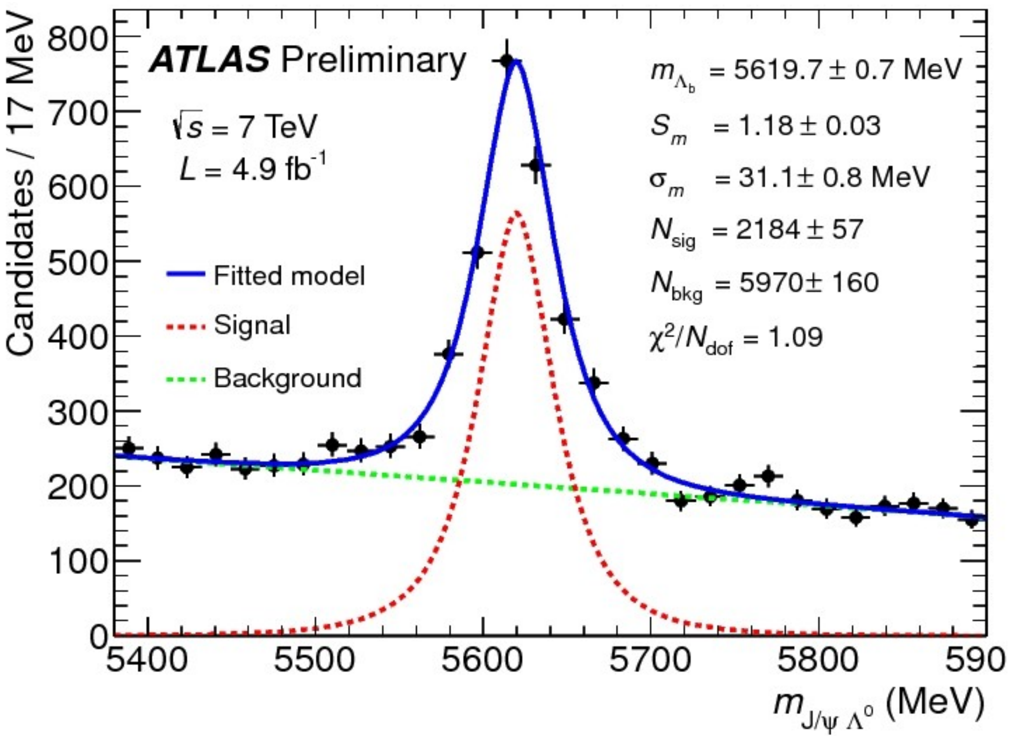

$$\tau_{\Lambda_b} = 1.449 \pm 0.036(\mathrm{stat}) \pm 0.017(\mathrm{syst})\ \mathrm{ps}$$

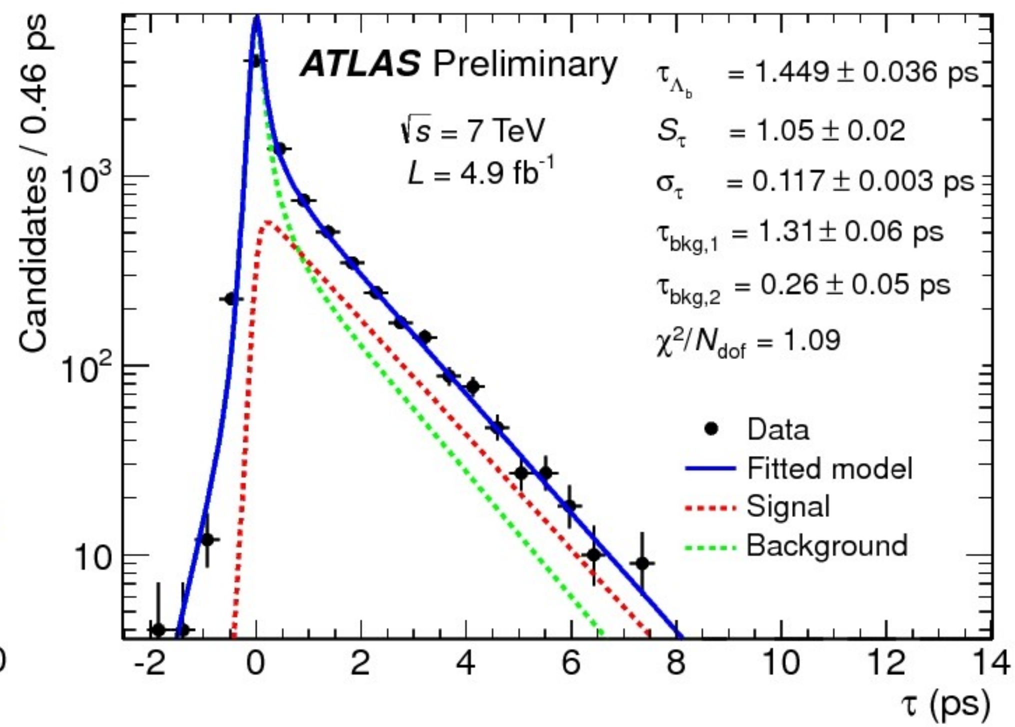

$$R = \tau_{\Lambda_b}/\tau_{B_d} = 0.960 \pm 0.025(\mathrm{stat}) \pm 0.016(\mathrm{syst})$$

B-lifetime measurements

- lifetimes measurements are the foundation for more complex measurements and selections (oscillations, mixing, $\Delta\Gamma$, β_s, rare decays etc.)

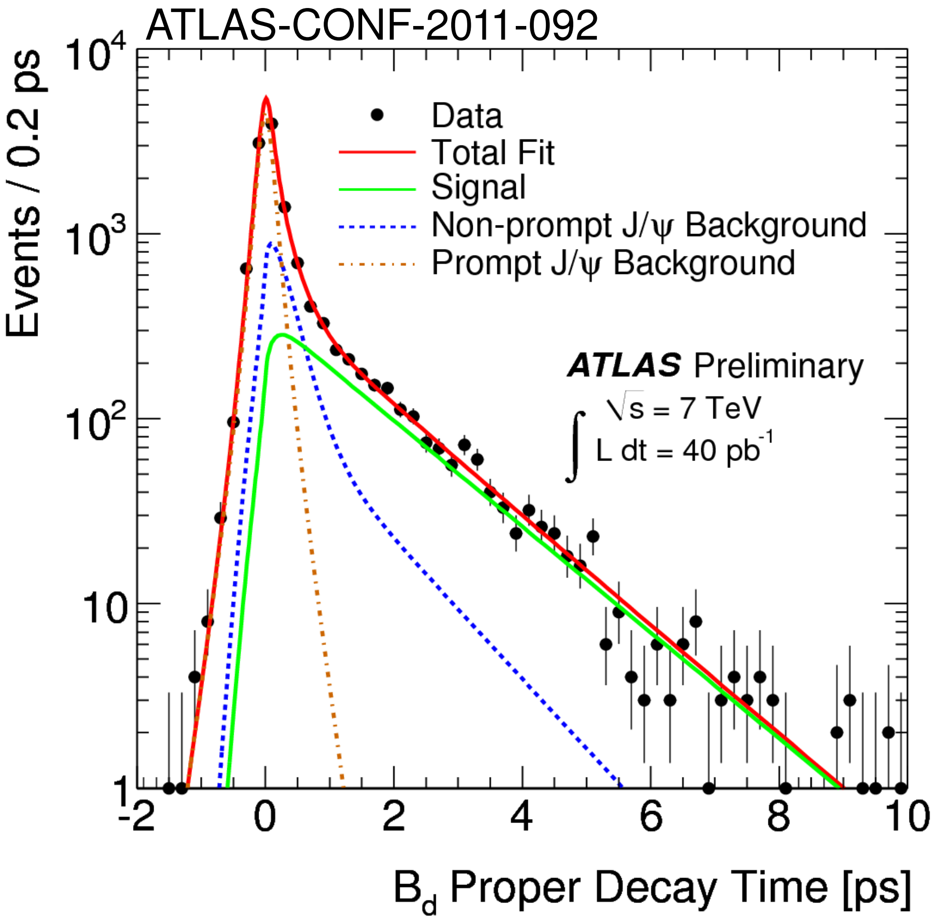

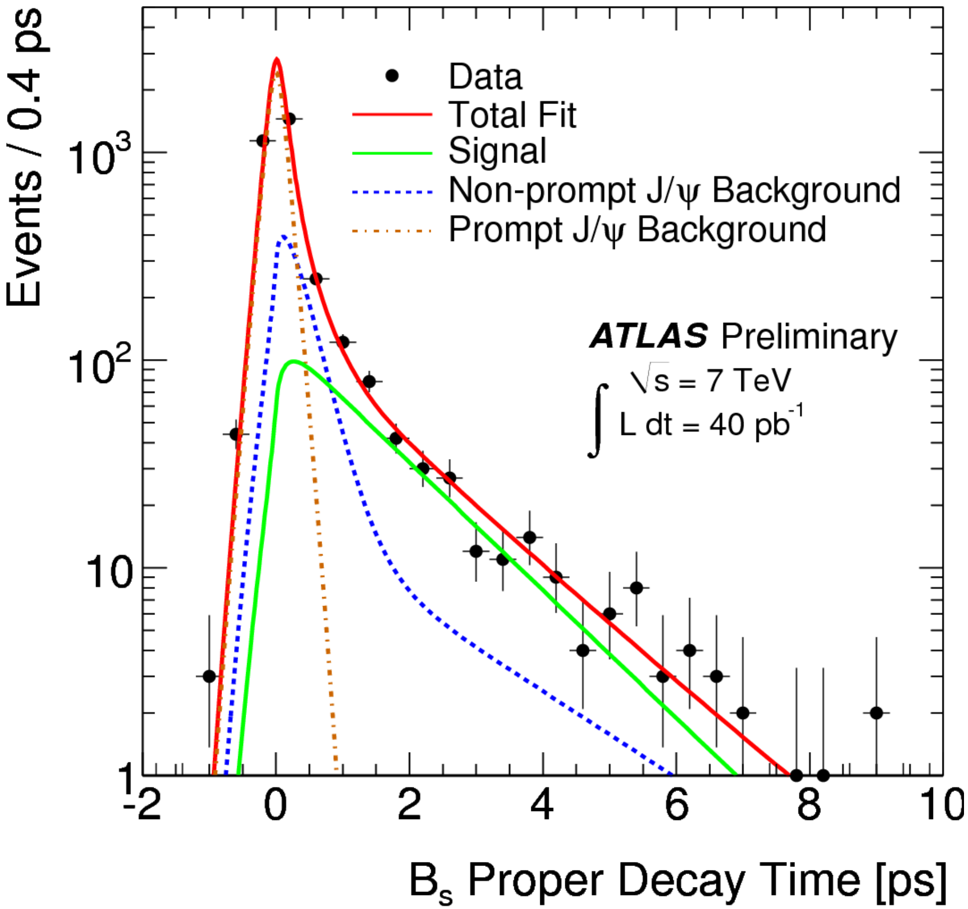

consistent with PDG

$$m_{B_d} = (5279.0 \pm 0.8)\,\mathrm{MeV}$$
$$\sigma_m = (34.3 \pm 0.9)\,\mathrm{MeV}$$
$$\tau_{B_d} = (1.51 \pm 0.04 \pm 0.04)\,\mathrm{ps}$$

$$m_{B_s} = (5363.7 \pm 1.2)\,\mathrm{MeV}$$
$$\sigma_m = (24.8 \pm 1.2)\,\mathrm{MeV}$$
$$\tau_{B_s} = (1.41 \pm 0.08 \pm 0.05)\,\mathrm{ps}$$

search for rare decays: $B_{(s)} \rightarrow \mu\mu$

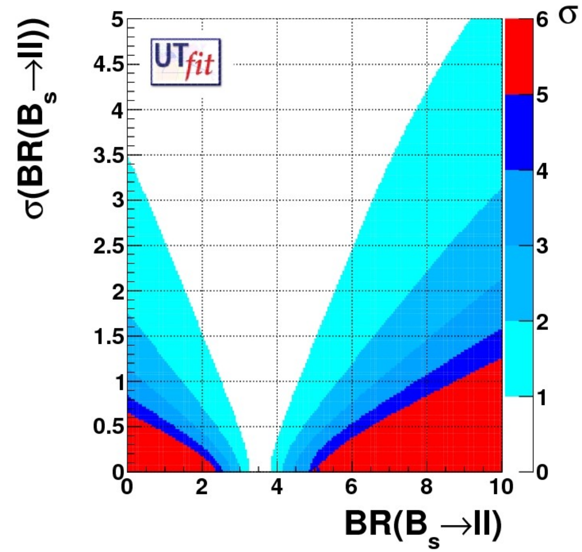

- flavour changing neutral currents (FCNC) are
•highly suppressed in the Standard Model
  - expected $B_s \rightarrow \mu\mu$ SM branching ratio:
    $(3.2 \pm 0.2)\ 10^{-9}$
    Buras et al., Phys.Lett. B694 (2011) 402
    $(3.5 \pm 0.3)\ 10^{-9}$
    UTfit prediction

- B to μμ branching ratio might be substantially enhanced by coupling to non-SM particles
  - being the SM well under control this channel provides a powerful method to peek into NP

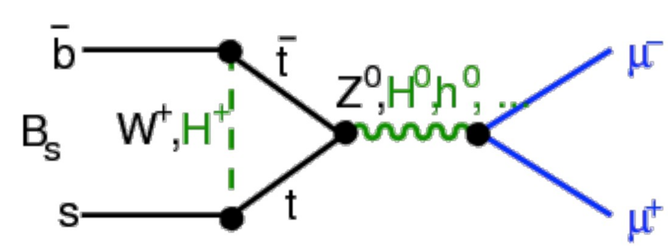

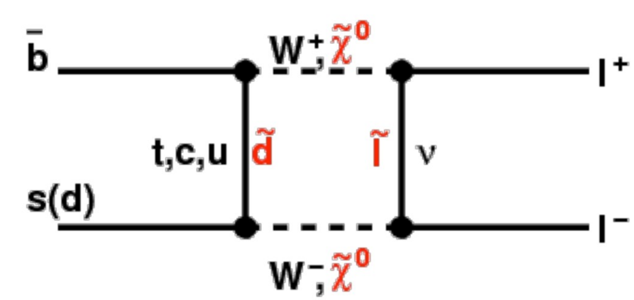

- orthogonal search for physics beyond the standard model
  - can reach higher scales wrt to the direct search

analysis strategy @ ATLAS:

Phys.Lett. B713 (2012) 387

- **Integrated luminosity 2.4 fb^{-1} used**
- **Relative BR measurement:**
  - partial cancellation of uncertainties: on luminosity, cross-section, ..
  - reference channel ($B^{\pm} \to J/\psi K^{\pm}$, $J/\psi \to \mu^+\mu^-$)
  - blind analysis: signal region ± 300 MeV around B_s
  - limit placed using CLs method

2.4fb^{-1}

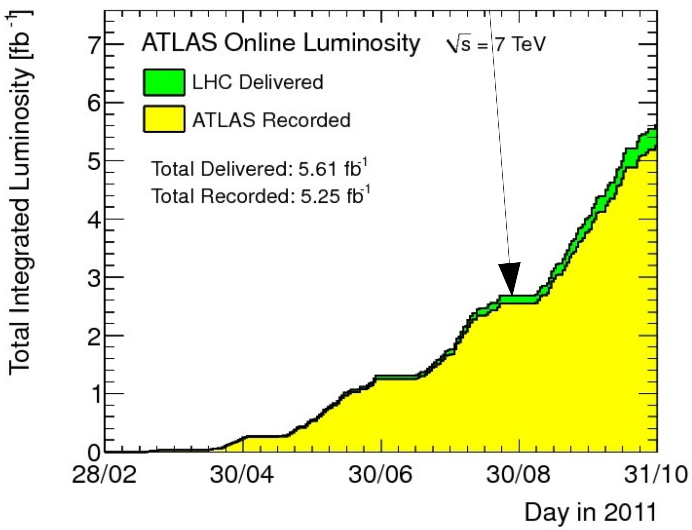

$$BR(B_s \to \mu\mu) = N_{B_s\to\mu\mu}\frac{1}{N_{B^{\pm}\to J/\psi K^{\pm}}} BR(B^{\pm} \to J/\psi K^{\pm}) \frac{f_u}{f_s} \frac{\varepsilon_{B^{\pm}\to J/\psi K^{\pm}}}{\varepsilon_{B_s\to\mu\mu}} \frac{A_{B^{\pm}\to J/\psi K^{\pm}}}{A_{B_s\to\mu\mu}}$$

- **Signal extraction:**
  - event count in "signal region"
  - "subtraction" of sidebands: interpolation from 50% of sidebands (even events)
- **Signal-background discrimination:**
  - selection based on 14 variables
  - multivariate analysis (BDT)
  - 50% of sidebands to model background (odd events)

Phys.Lett. B713 (2012) 387

analysis strategy @ ATLAS:

Relative BR measurement:

- partial cancellation of uncertainties:
  on luminosity, cross-section, ..
- reference channel ($B^{\pm} \to J/\psi K^{\pm}$, $J/\psi \to \mu+\mu-$)
- blind analysis: signal region ± 300 MeV around B_s mass blinded
- limit placed using CLs method

$$BR(B_s \to \mu\mu) = N_{B_s\to\mu\mu} \frac{1}{N_{B^{\pm}\to J/\psi K^{\pm}}} BR(B^{\pm} \to J/\psi K^{\pm}) \frac{f_u}{f_s} \frac{\varepsilon_{B^{\pm}\to J/\psi K^{\pm}}}{\varepsilon_{B_s\to\mu\mu}} \frac{A_{B^{\pm}\to J/\psi K^{\pm}}}{A_{B_s\to\mu\mu}}$$

Efficiencies & acceptances

- Derived from simulation (“calibrated” on data)
  $\varepsilon \cdot A = (N_{\text{reconstructed and selected}}/N_{\text{generated}})$
- Reference channel ($B^{\pm} \to J/K^{\pm}$) selected with as-close-as-possible selection

BR of the reference channel and relative production rate f_u/f_s

- taken from PDG and the latest LHCb results

background composition

- **continuum:**
  - dominated by non-resonant bb production with $\mu\mu X$ final states → real muons
  - smooth shape in the di-muon mass
  - 14 discriminating variables used in a boosted decision tree (BDT) to discriminate against this background
  - measured by interpolation from sideband data into the signal region

B_s signal (MC) vs background (sidebands)

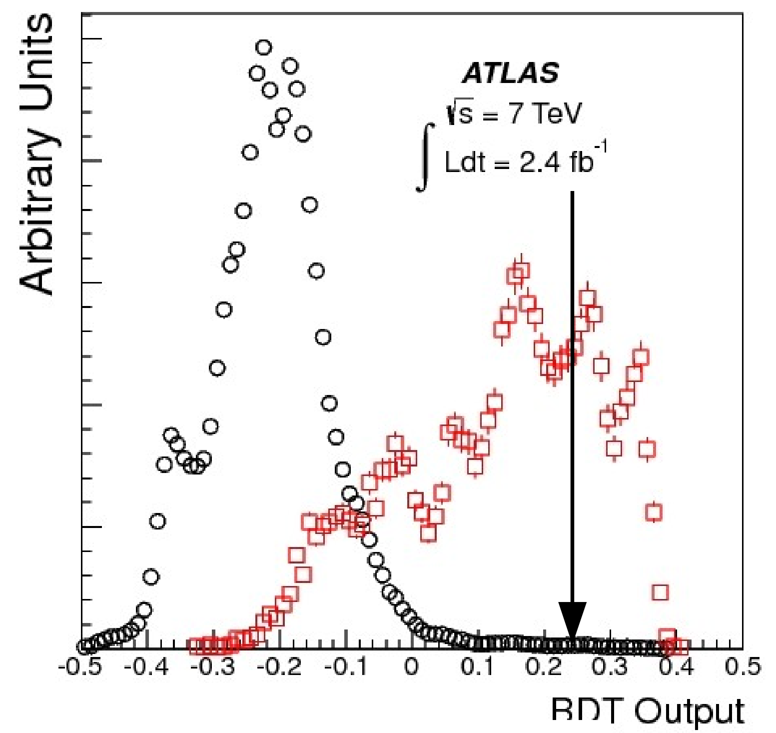

- **resonant**:
  - B → hh, with hadrons misidentified as muons
  - mainly $B \rightarrow K^+\pi^-/\pi^+\pi^-$ decays
  - BR x (fake rate) ≈ 10^{-9} close to the SM B_s to $\mu\mu$ BR
  - similar decay topology → hard to suppress
  - contribution estimated from MC: currently still quite small

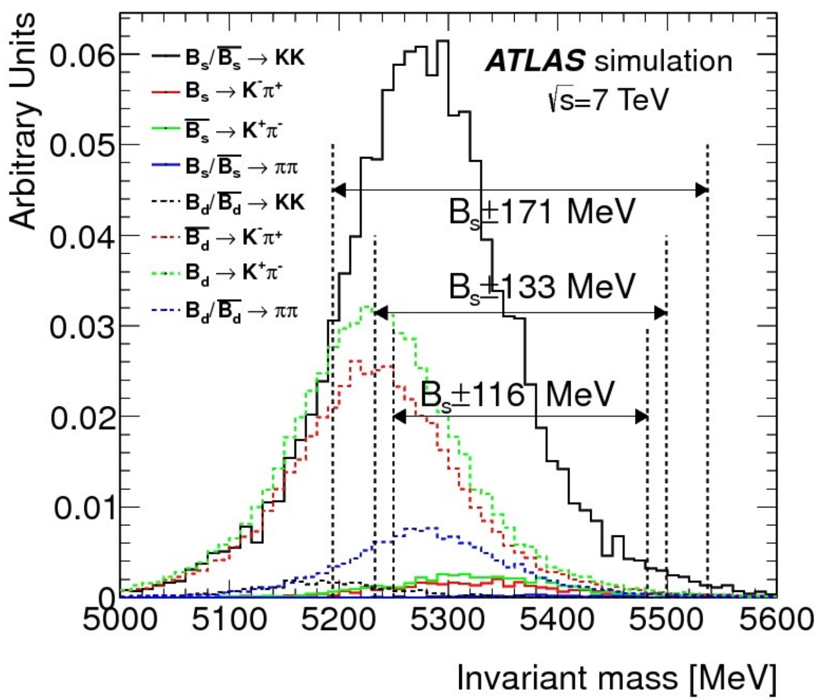

Phys.Lett. B713 (2012) 387

signal and reference yields

- keep selections synchronised and same BDT to minimise systematics
- inclusion of per-event mass resolution in the fit

$\|\eta\|_{\max}$ Range	0–1.0	1.0–1.5	1.5–2.5
$B^{\pm} \to J/\psi K^{\pm} \to \mu^{+}\mu^{-}K^{\pm}$	4300	1410	1130
statistical uncertainty	±1.6%	±2.8%	±3.0%
systematic uncertainty	±2.9%	±7.4%	±14.1%

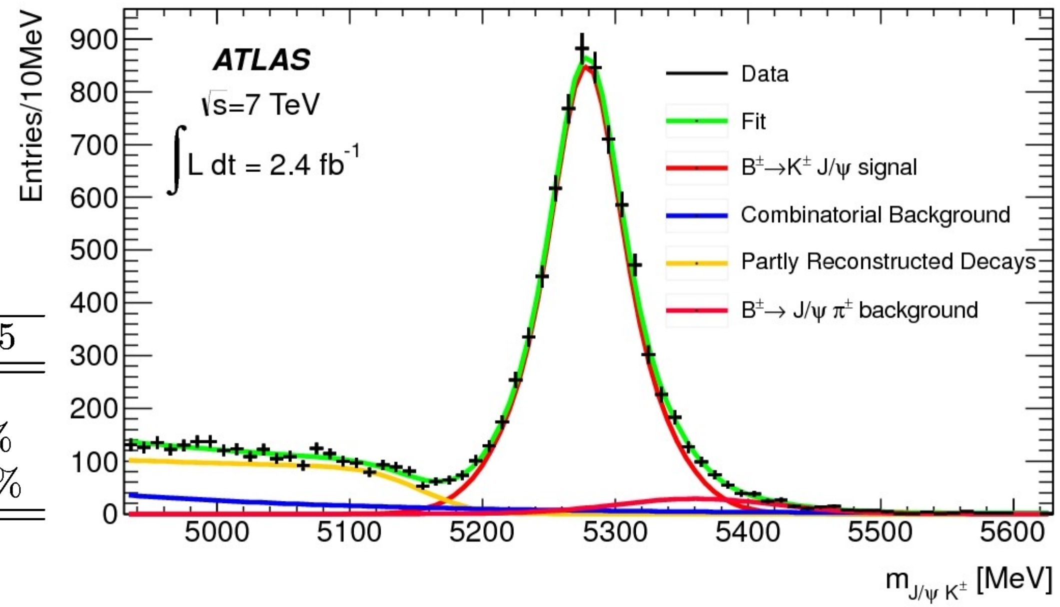

- **opening the signal box**

	$\|\eta\| < 1.0$	$1.0 < \|\eta\| < 1.5$	$1.5 < \|\eta\| < 2.5$
Even events in sidebands	**5**	**0**	**2**
Expected background events in SR	**3.86**	**0**	**2.28**
Expected resonant background	**0.1**	**0.06**	**0.08**
Observed events in SR	**2**	**1**	**0**

sidebands

optimized search window

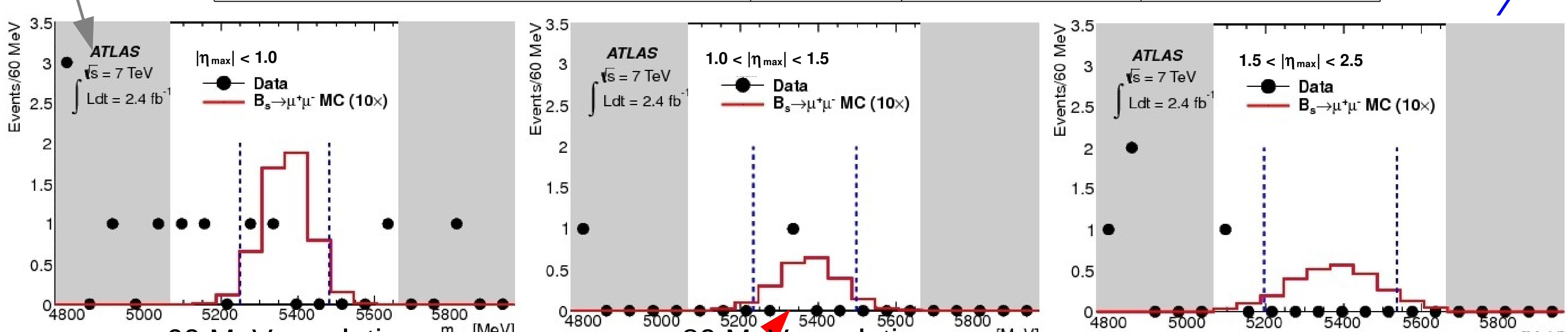

60 MeV resolution

80 MeV resolution

110 MeV resolution

signal peak 10 times enhanced

upper limit

- Upper limit extracted with modified frequentist (CLs) approach
- Limit expectation at 95% CL
- Even-event sidebands: **2.3 10^{-8}**
- All mass resolution bins merged (for comparison): **2.9 10^{-8}**
- Observed limit at 95% CL: **2.2 10^{-8}**

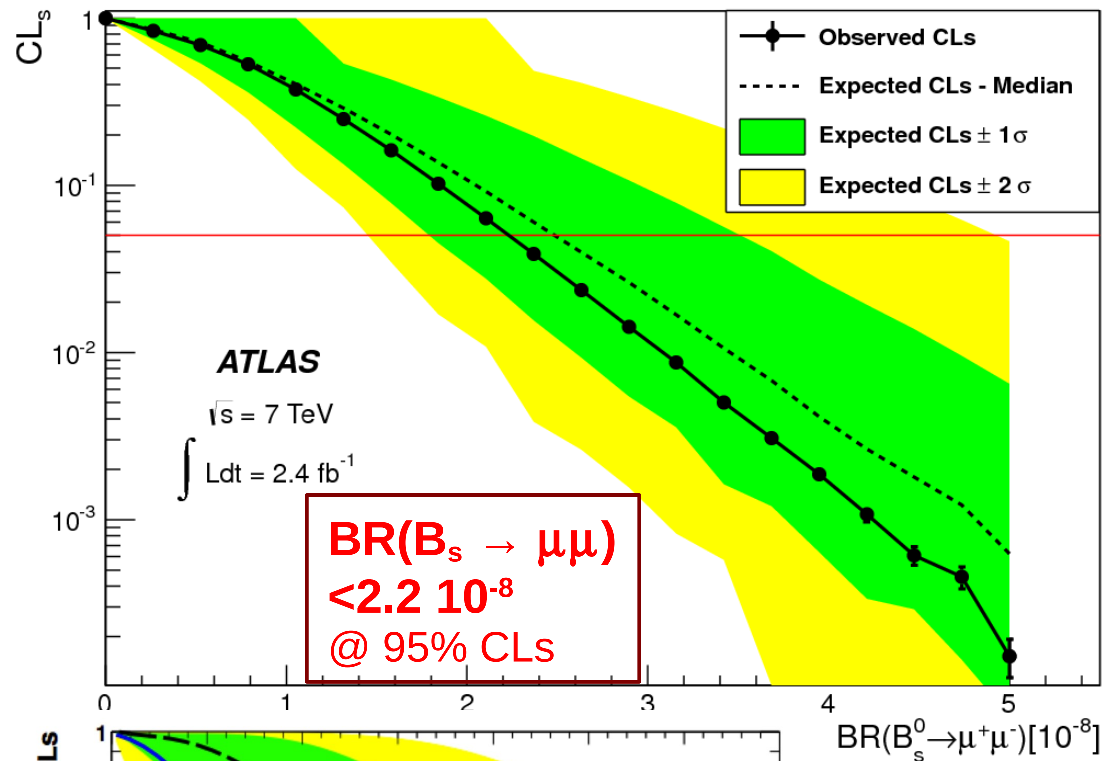

- ATLAS result combined with CMS and LHCb
- Observed limit at 95% CL: **4.2 10^{-9}**

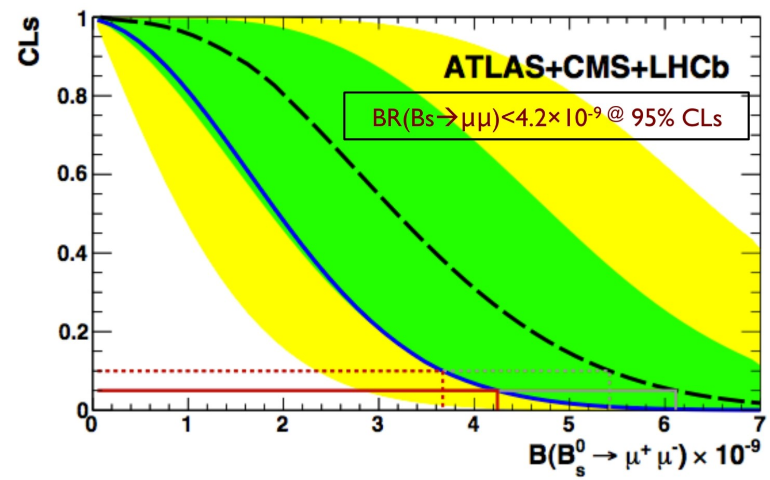

ATLAS-CONF-2012-061

Mode	Limit	ATLAS	CMS	LHCb 2010	LHCb 2011	Combined
$B_s^0 \to \mu^+\mu^-$ (10^{-9})	Bkg Only	23	(3.6)	65	3.4	2.3
	Bkg+SM		8.4		7.2	6.1
	Obs	22	7.7 (7.2)	56	4.5	4.2

Compatible with SM signal within 1σ ($1\text{-}CL_{s+b}$=84%)
p-value bkg-only hypothesis ($1\text{-}CL_b$): 5%

$\Delta\Gamma_s$ and ϕ_s measurement from $B_s \to J/\psi\phi$

- The time evolution of the meson B_S and $\overline{B}_S$ is described by the superposition of B_H and B_L states, with masses $m_S \pm \Delta m_S/2$ and lifetimes $\Gamma_S \pm \Delta\Gamma_S/2$.

  These states deviate from defined values CP = ± 1, as described in the SM by the mixing phase ϕ_S ($\phi_S = -2\beta_S$),

  SM prediction (fit): $\phi_S = -0.0368 \pm 0.0018$ *rad*

  $\Delta\Gamma_S = 0.082 \pm 0.021\ ps^{-1}$

  New Physics can contribute to ϕ_S, and change the ratio $\Delta\Gamma_S/\Delta m_S$.

- In general, the decay to a final state that is coupled to B_S and/or $\overline{B}_S$, exhibits fast oscillations driven by Δm_S. Interference between amplitudes for both states generates CP violation, and conveys information on ϕ_S .

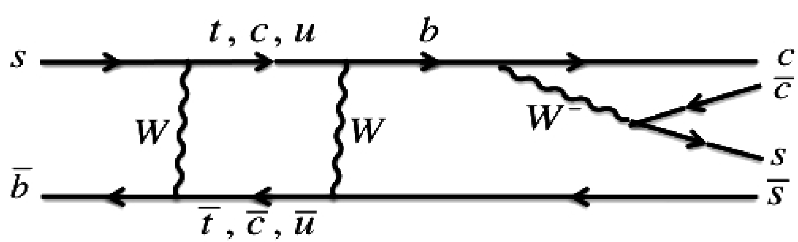

Decay amplitude with mixing (φ_s)

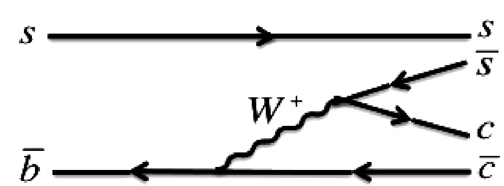

Amplitude with direct decay

If $\overline{B}$/B flavour at production is not determined (not tagged), the fast oscillations cannot be observed, but interference terms remain if the final state is described by a superposition of amplitudes of different CP values.

angular analysis in $B_s \to J/\psi\phi$

- In the decay $\overline{B}_S(B_S) \to J/\psi\phi \to l^+l^- K^+K^-$ different components in the angular-distributions amplitudes correspond to CP = +1 or –1
- The "transversity angles" are used to describe the angular distributions

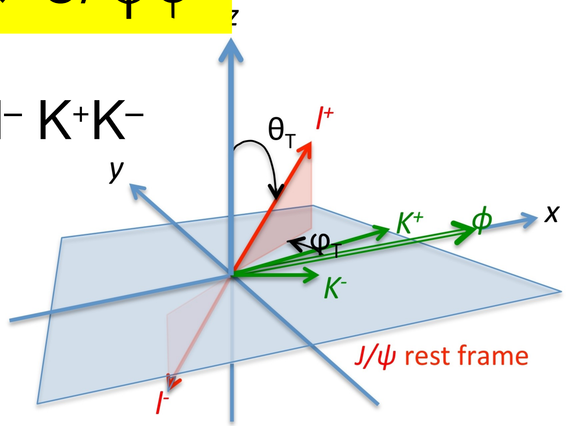

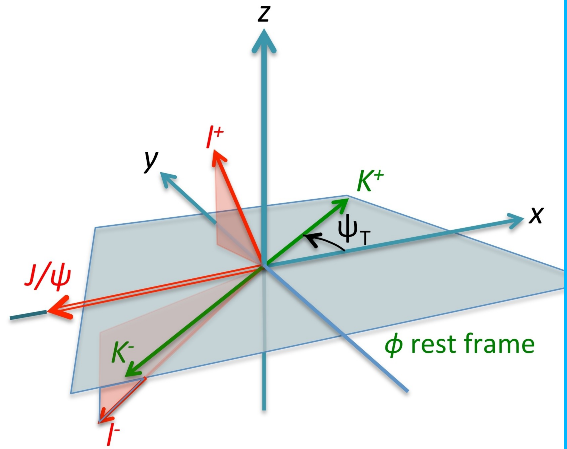

- Analysis using data collected in 2011, corresponding to 4.7 fb^{-1}
- Signal extracted from a maximum likelihood fit:

the signal with amplitude f_s

$$\ln \mathcal{L} = \sum_{i=1}^{N} \{ w_i \cdot \ln(f_s \cdot \mathcal{F}_s(m_i, t_i, \Omega_i) + f_s \cdot f_{B^0} \cdot \mathcal{F}_{B^0}(m_i, t_i, \Omega_i) + (1 - f_s \cdot (1 + f_{B^0}))\mathcal{F}_{bkg}(m_i, t_i, \Omega_i))\} + \ln P(\delta_\perp)$$

the prompt and non-prompt combinatorial background described with empirical angular distribution. (No K-π discrimination.)

w_i describes a small trigger inefficiency (~1%)..

the background due to $B^0 \to J/\psi K^{*0}$ and $B^0 \to J/\psi K\pi$ with amplitude f_{B0}

results of the fit

$$\ln\ \mathcal{L} = \sum_{i=1}^{N}\{w_i \cdot \ln(f_s \cdot \mathcal{F}_s(m_i, t_i, \Omega_i) + f_s \cdot f_{B^0} \cdot \mathcal{F}_{B^0}(m_i, t_i, \Omega_i) + (1 - f_s \cdot (1 + f_{B^0}))\mathcal{F}_{bkg}(m_i, t_i, \Omega_i))\} + \ln P(\delta_\perp)$$

projection on B_s mass and proper decay time

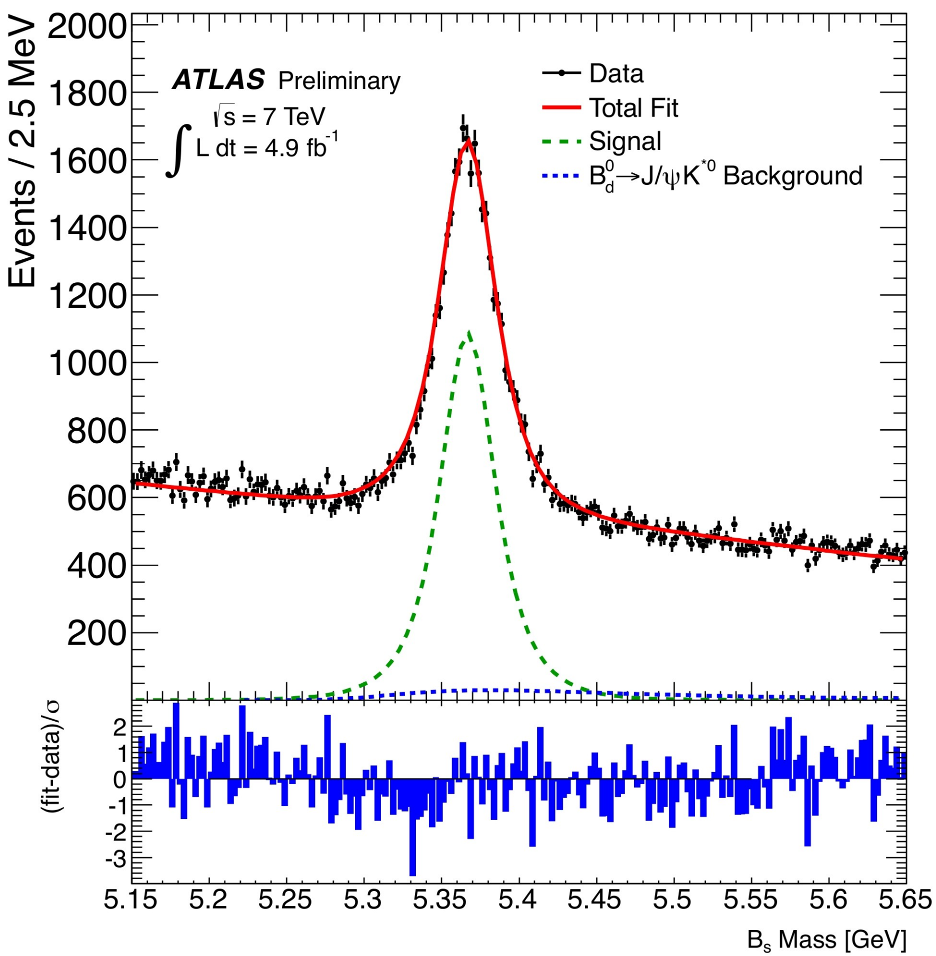

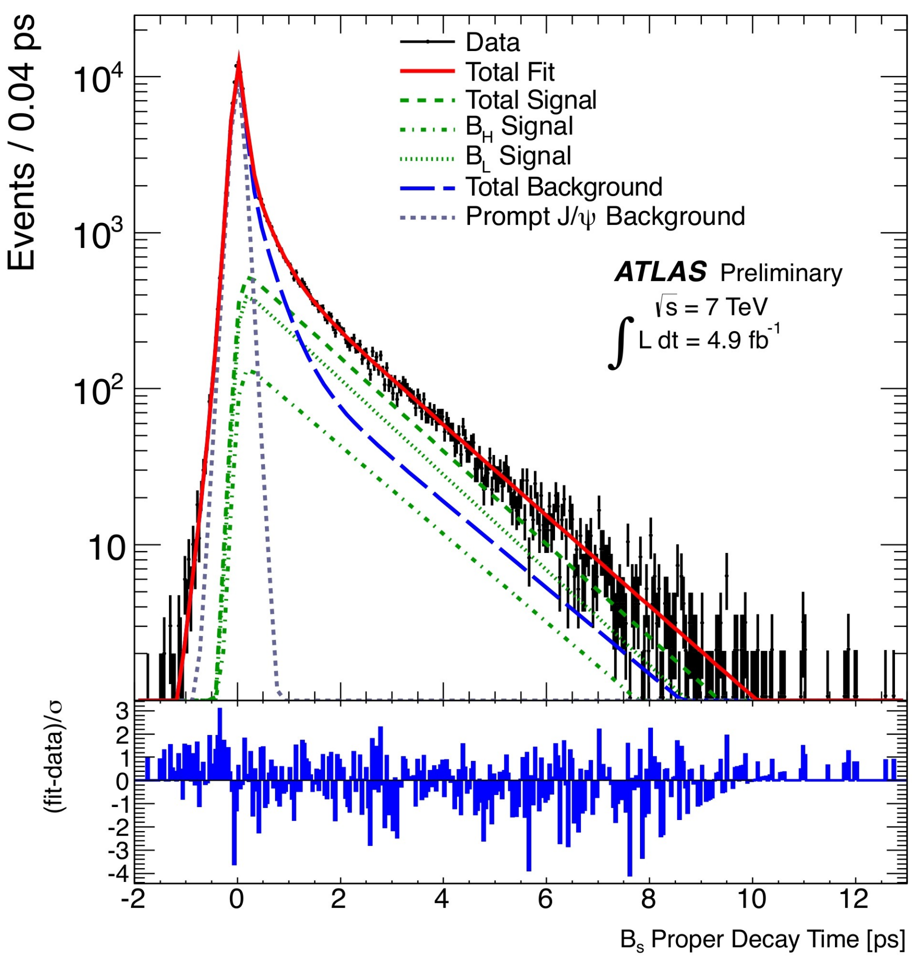

result for ϕ_S and $\Delta\Gamma_S$ in $B_s \to J/\psi\phi$

- The $B_S \to J/\psi\ \phi$ term in the likelihood is invariant under the transformations:

$$\{\phi_s, \Delta\Gamma_s, \delta_\perp, \delta_\parallel\} \rightarrow \{\pi - \phi_s, -\Delta\Gamma_s, \pi - \delta_\perp, 2\pi - \delta_\parallel\}$$

$$\{\phi_s, \Delta\Gamma_s, \delta_\perp, \delta_\parallel\} \rightarrow \{-\phi_s, \Delta\Gamma_s, \pi - \delta_\perp, 2\pi - \delta_\parallel\}$$

The ATLAS analysis favours values of ϕ_S close to 0 (π), for which an untagged analysis is scarcely sensitive to the phase $\delta_\perp$

so we constrain the value of $\delta_\perp$ to 2.95 ± 0.39 rad [from LHCb]

the four minima of the likelihood do not overlap, only one of them is compatible with previous measurements, and we show the result for that minimum.

Parameter	Value	Statistical uncertainty	Systematic uncertainty
ϕ_s(rad)	0.22	0.41	0.10
$\Delta\Gamma_s(\mathrm{ps}^{-1})$	0.053	0.021	0.008
$\Gamma_s(\mathrm{ps}^{-1})$	0.677	0.007	0.004
$\|A_0(0)\|^2$	0.528	0.006	0.009
$\|A_\parallel(0)\|^2$	0.220	0.008	0.007
$\|A_S(0)\|^2$	0.02	0.02	0.02

Correla1on coefficients

	ϕ_s	$\Delta\Gamma_s$	Γ_s	$\|A_0(0)\|^2$	$\|A_\parallel(0)\|^2$	$\|A_S(0)\|^2$
ϕ_s	1.00	−0.13	0.38	−0.03	−0.04	0.02
$\Delta\Gamma_s$		1.00	−0.60	0.12	0.11	0.10
Γ_s			1.00	−0.06	−0.10	0.04
$\|A_0(0)\|^2$				1.00	−0.30	0.35
$\|A_\parallel(0)\|^2$					1.00	0.09
$\|A_S(0)\|^2$						1.00

result for ϕ_s and $\Delta\Gamma_s$ in $B_s \to J/\psi\phi$

Likelihood profiles in the $\phi_s - \Delta\Gamma_s$ plane

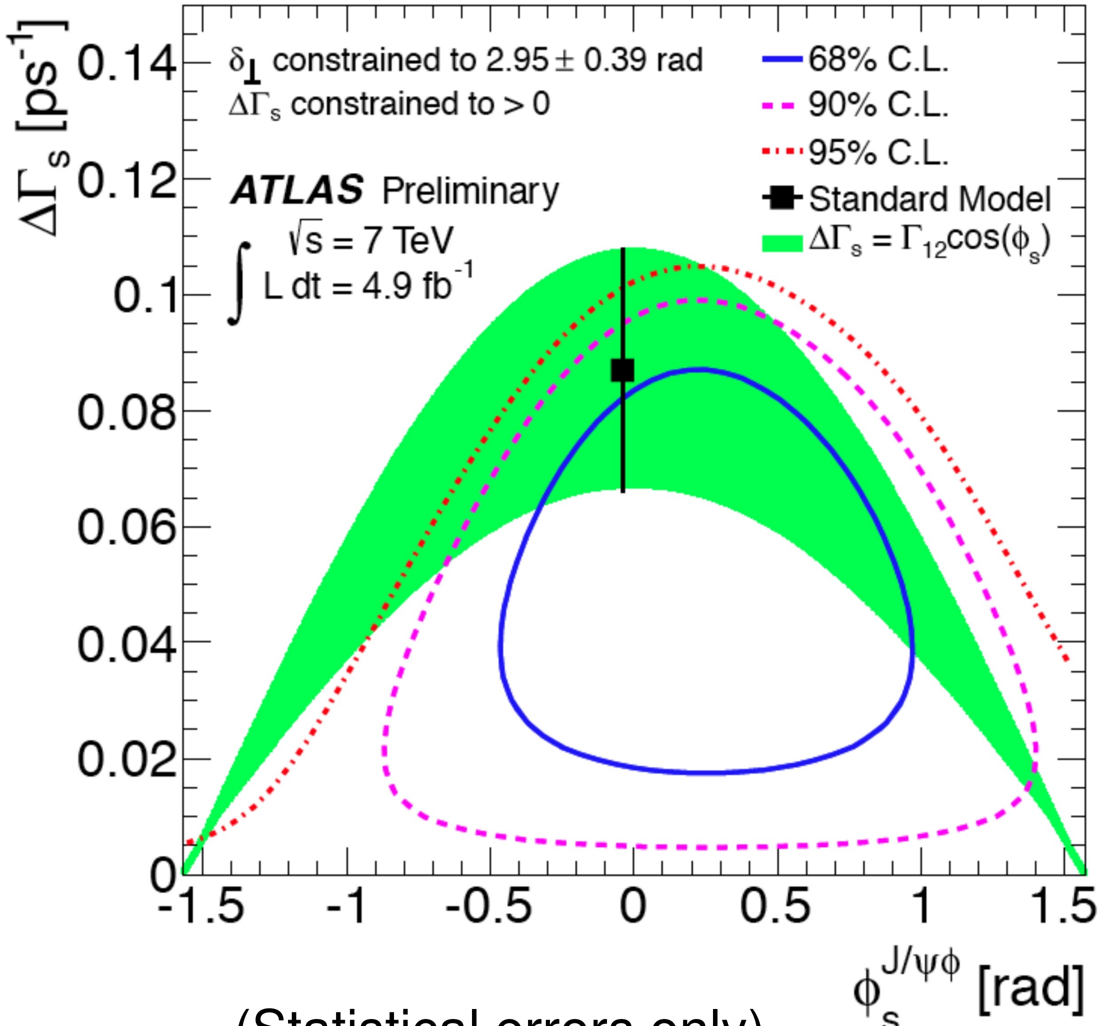

(Statistical errors only)

Agreement with the SM prediction

comparison with other experiments

on the $\phi_S - \Delta\Gamma_S$ plane

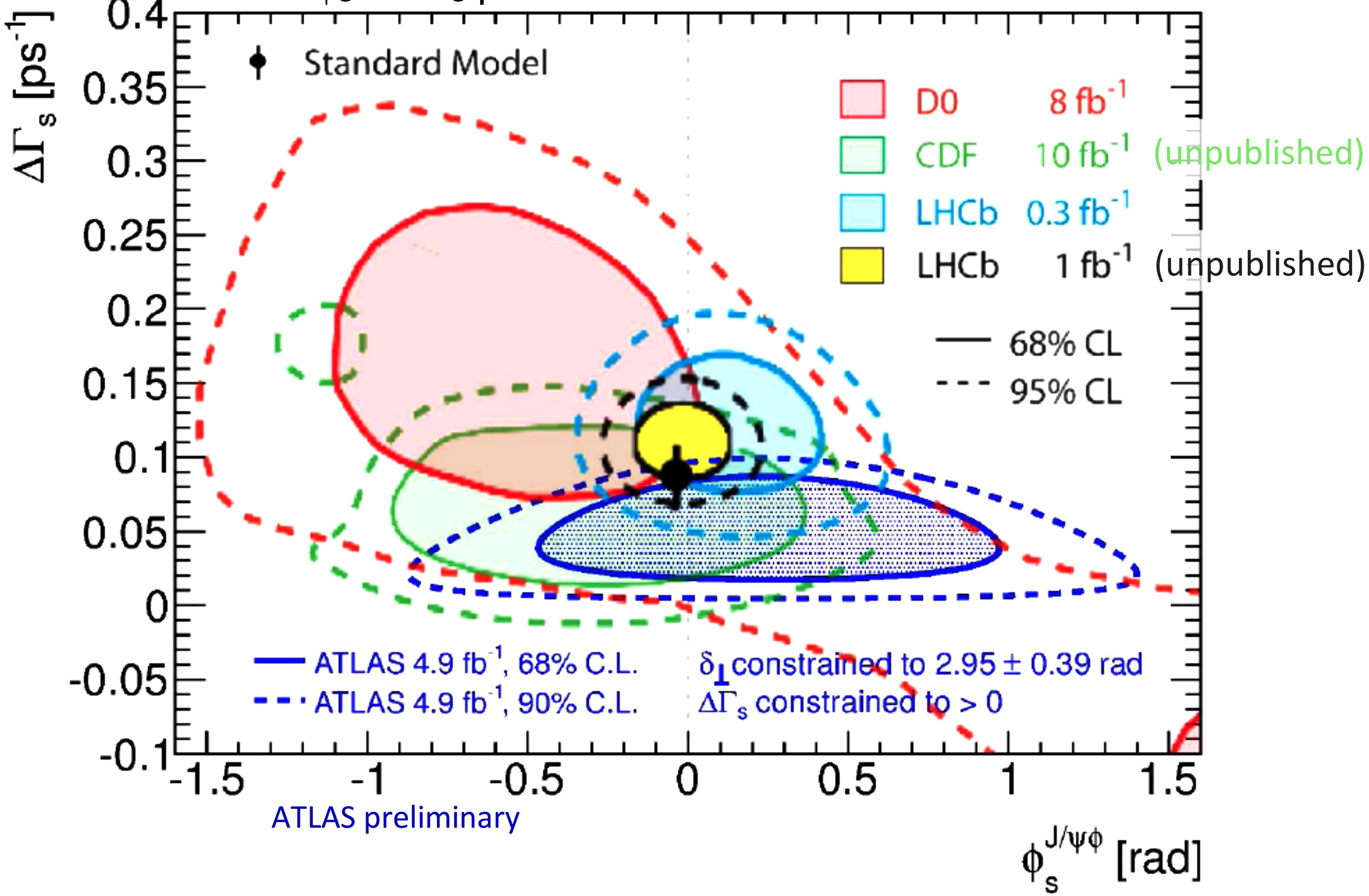

conclusions

- Heavy Quarkonium:
  - it continues to challenge current understanding
  - data and theory gap reducing.
  - ATLAS has measured/observed:
    - J/ψ: inclusive, prompt and non-prompt differential cross-sections
    - χ_c observed through radiative decays to J/ψ
    - $\chi_b(1P)$ and $\chi_b(2P)$ observed through radiative decays to $\Upsilon(1S)$
    - First observation of $\chi_b(3P)$ state decaying to $\Upsilon(1S)$ and $\Upsilon(2S)$

- B physics:
  - Benchmarks and standard-candles well assessed
  - ATLAS has measured:
    - First analysis on rare decay $B_s \to \mu\mu$
    - Decay time and angular distributions have been studied in $B_s \to J/\psi\ \phi$ events without flavour tagging.

near future

- Heavy Quarkonium:
  - Spin-alignment measurement will reduce a dominant source of uncertainty.
  - Measurements of:
    - Υ(1,2,3S) and ψ(2S)($\rightarrow \mu\mu$ and $\rightarrow \mu\mu\pi\pi$) production cross-sections
    - ψ(2S) to J/ψ production ratios, di-onia production
    - and cross-sections of $\chi_{c/b}$ systems,

    will provide important input on the underlying mechanisms of Heavy Quarkonium near the strong decay threshold.

- B physics:
  - Improvements, updates and new analyses in the pipeline
  - Lots of statistics already on tape
    - update the rare B $\rightarrow \mu\mu$ decay search
    - B $\rightarrow \mu\mu K^*$ also being looked into
    - CP violation in $B_S \rightarrow J/\psi\, \phi$ events with flavour tagging.

backup

Υ: fiducial cross-section

- This analysis uses 1.13 pb^{-1}
- The cross-section of Υ(1S) is measured as a function of the p_T in two bins of rapidity (barrel |η|< 1.2 and endcaps 1.2 < |η| <2.4)
- Cross section measured within ATLAS fiducial volume – no acceptance corrections, factors out polarization uncertainty
- Background from opposite side μ + track sample
- Likelihood fit to Υ(1,2,3S) and background templates

Phys.Lett.B 705 (2011) 9-27

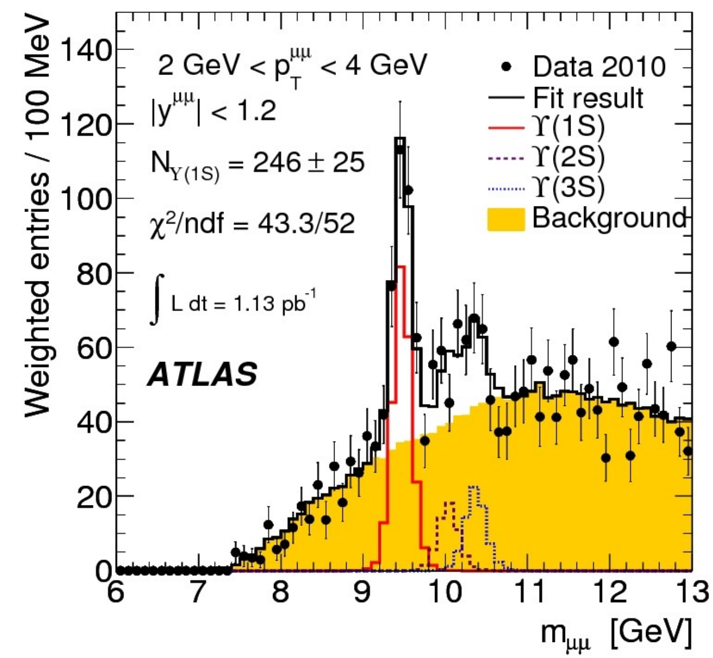

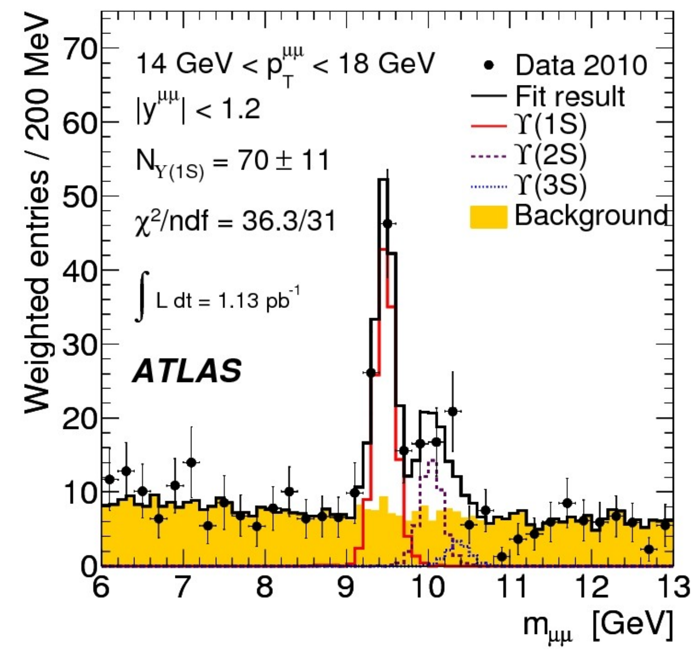

Backgrounds more significant than in J/ψ, larger and more complex!
Use OS/SS μ+trk data and HF MC to model

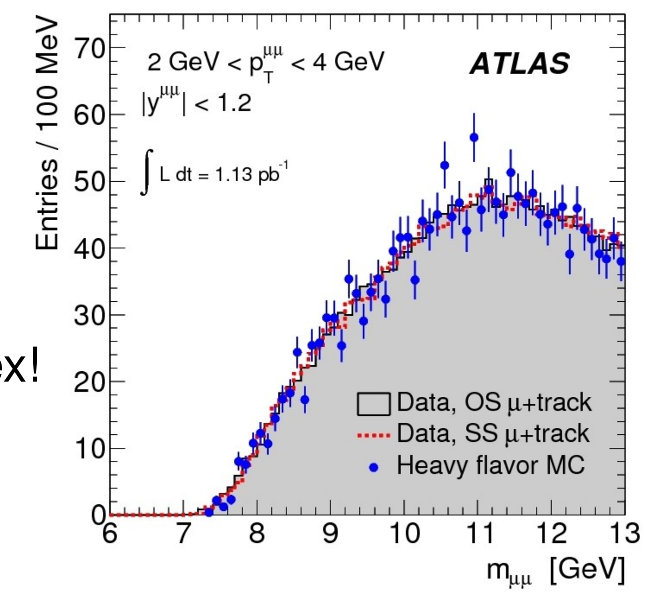

Υ: fiducial cross-section

Phys.Lett.B 705 (2011) 9-27

- Results are not corrected for acceptance:
  - defined within muon kinematics (p_T > 4 GeV, |η|<2.5)
  - removes spin-alignment uncertainty

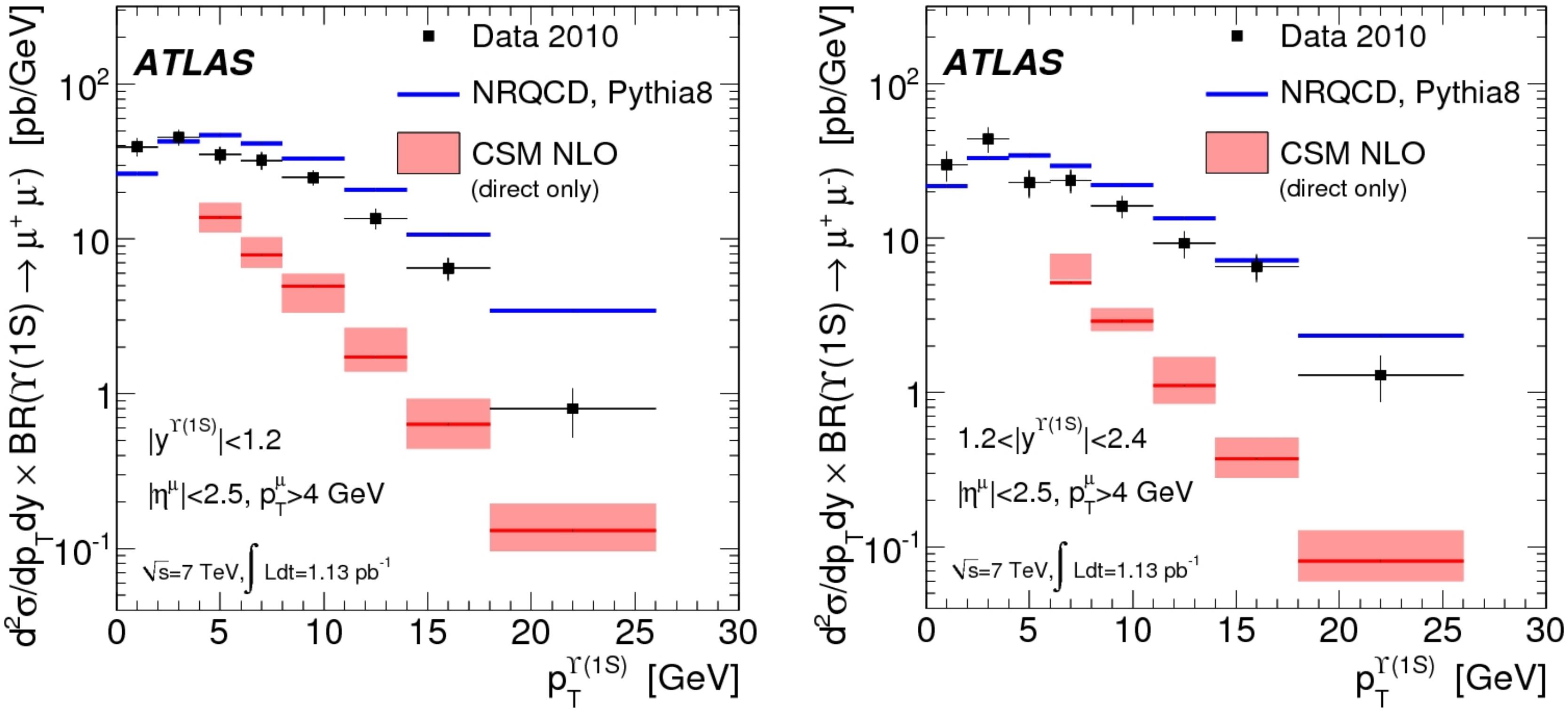

- Colour Singlet Model prediction is low, but contains no feed down from higher order states (NLO only)
- NRQCD shows closer agreement (within ~2x), although shape is not matched.

J/ψ: spin-alignment

Acceptance: probability that J/ψ survives muon cuts
However, acceptance depends on spin alignment
not yet well measured under LHC conditions

Isotropic distribution taken as central assumption

Take five specific working-point scenarios
use an envelope of additional uncertainty on central value

Relative uncertainty between different scenarios reduces at higher p_T.

analysis strategy @ ATLAS:

- **Relative BR measurement:**
  - partial cancellation of uncertainties:
    on luminosity, cross-section, ..
  - reference channel ($B^{\pm} \rightarrow J/\psi K^{\pm}$, $J/\psi \rightarrow \mu+\mu-$)
  - blind analysis: signal region ± 300 GeV around B_s mass blinded
  - limit placed using CLs method

$$BR(B_s \to \mu\mu) = N_{B_s\to\mu\mu} \frac{1}{N_{B^\pm\to J/\psi K^\pm}} BR(B^\pm \to J/\psi K^\pm) \frac{f_u}{f_s} \frac{\varepsilon_{B^\pm\to J/\psi K^\pm}}{\varepsilon_{B_s\to\mu\mu}} \frac{A_{B^\pm\to J/\psi K^\pm}}{A_{B_s\to\mu\mu}}$$

Single Event Sensitivity (SES)

corresponds to the $B_s \rightarrow \mu^+\mu^-$ branching fraction which would yield one observed signal event in the data sample.

background composition

- **continuum:**
  - dominated by non-resonant bb production with μμX final states
  - real muons
  - smooth shape in the di-muon mass
  - limited MC statistics available in ATLAS
  - measured by interpolation from sideband data into the signal region

- **resonant**:
  - B → hh, with hadrons misidentified as muons
  - mainly B → $K^+\pi^-/\pi^+\pi^-$ decays
  - BR x (fake rate) ≈ 10^{-9} close to the SM B_s to μμ BR
  - similar decay topology → hard to suppress
  - contribution estimated from MC: currently still quite small

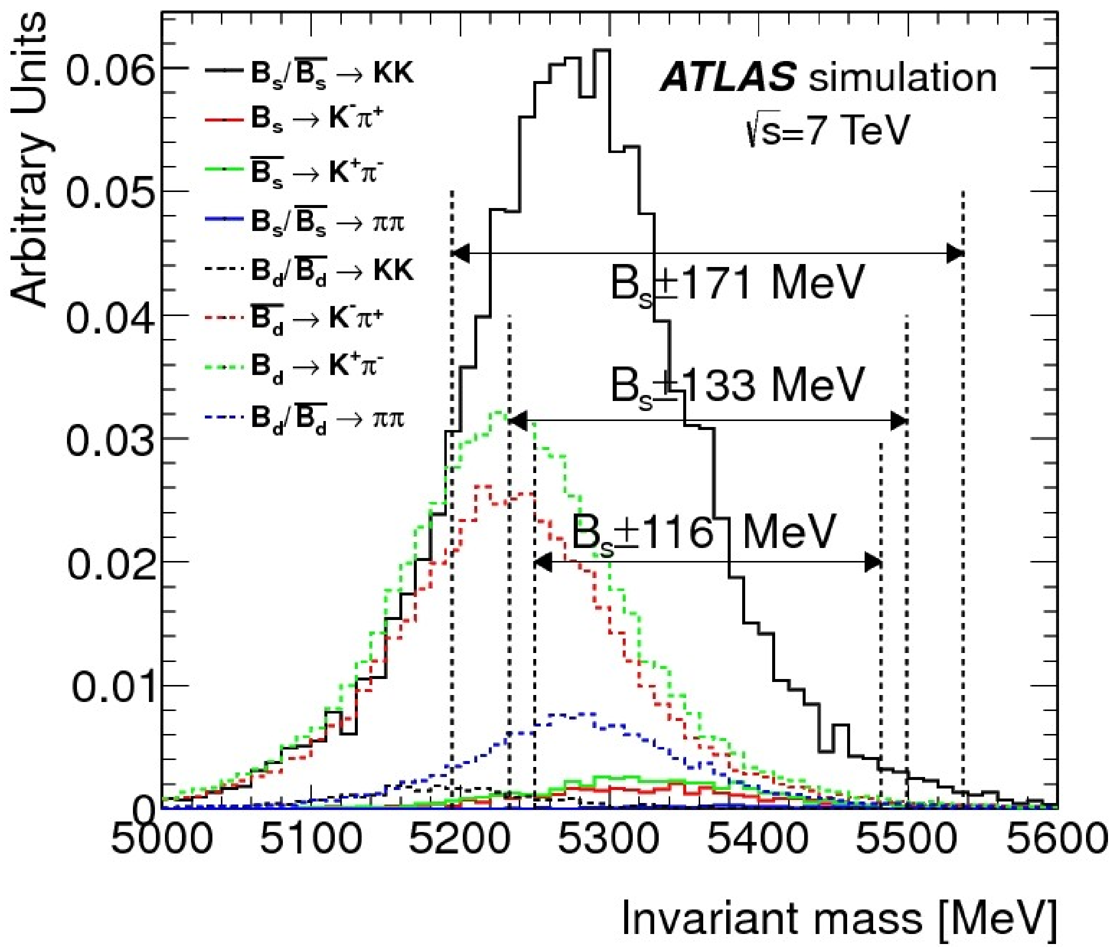

background composition

- **continuum:**
  - select events based on their decay topology
  - discriminating variables to distinguish between B and continuum
  - 14 variables identified and used in a boosted decision tree (BDT):

B_s signal (MC) vs **background (sidebands)**
⇒ clear separation

$B^{\pm}$ data (sideband subtracted)
vs MC (weighted) ⇒ good agreement

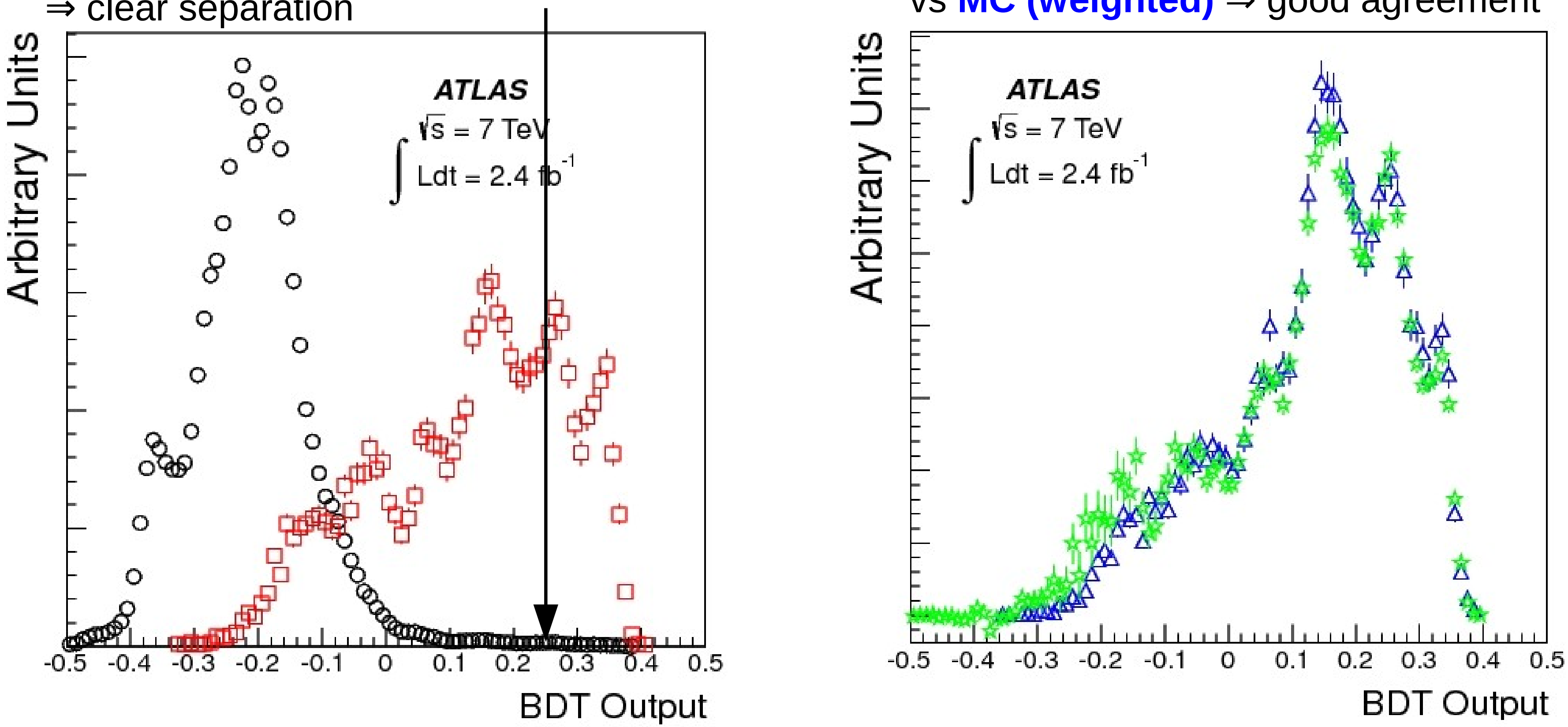

data-MC comparison for B to μμ

B meson kinematic variables weighted in MC to match distributions in data

Agreement verified on B± data (sideband subtracted):

Residual deviations for some variables
→ accounted for in systematics

Isolation variable cross-checked on $B_s \rightarrow J/\psi\phi$ control sample
→ no discrepancies between data and MC found

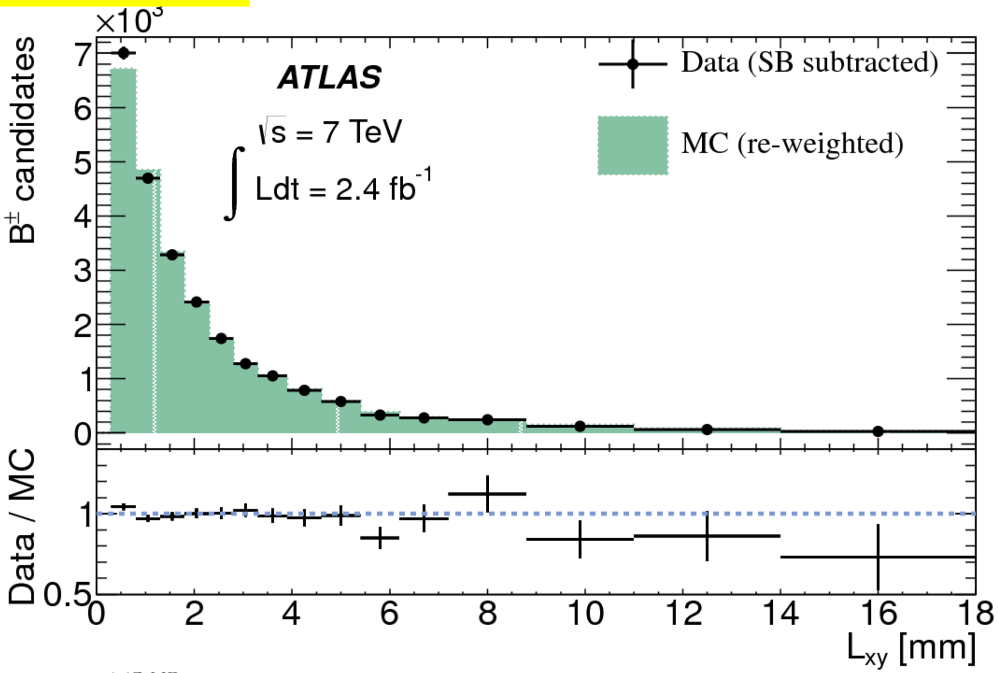

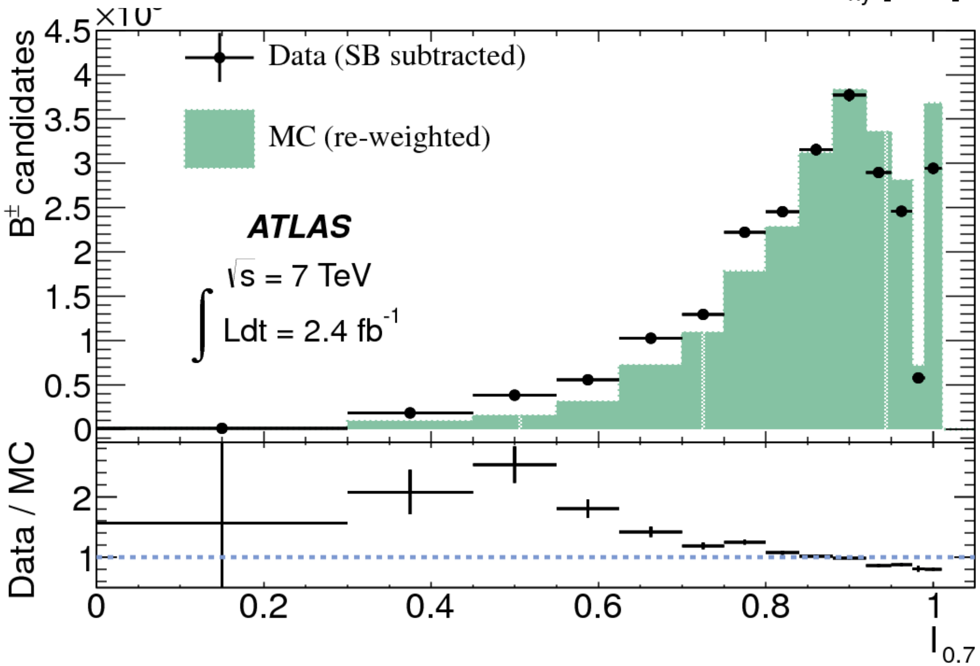

reconstruction and event selection

- 2, 3 or 4 prong vertex constraint depending on decay topology
- Primary Vertex selection:
  - the closest in z to the B candidate
  - Re-fit excluding B daughters
- Tracks:
  - At least 1 pixel, 6 SCT and 9 TRT hits (*good tracks*)
  - $|\eta| < 2.5$ and $p_T > 4$ (2.5) GeV for muons (kaons)
  - tracks from the tracking systems matched to muon spectrometer tracks
- B candidates: $p_T > 8$ GeV and $|\eta|<2.5$

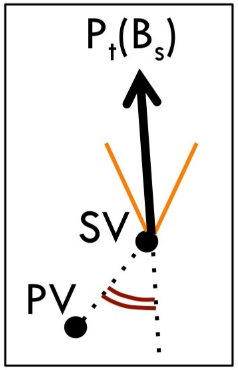

- select events based on their decay topology
- discriminating variables to distinguish between B and continuum events
- 14 variables identified and used in a boosted decision tree (BDT):
  - not correlated with invariant mass
  - highest discriminating power
  - highly correlated variables excluded

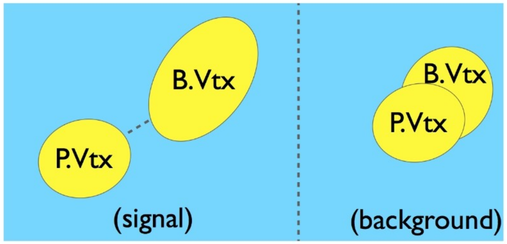

discriminating variables

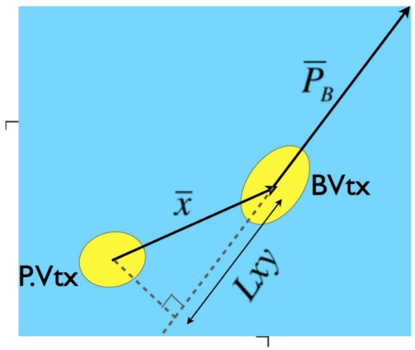

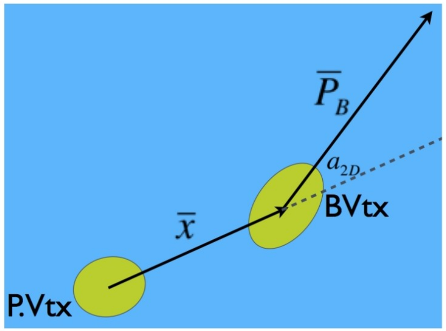

Exploit:

- Primary Vertex-Secondary Vertex separation: L_{xy}, $c\tau$ significance
- Symmetry of final state: pointing angle, d_0…
- Full reconstruction: pointing angle, D_{min}…
- B hadronization features: Isolation, p_T of the B…

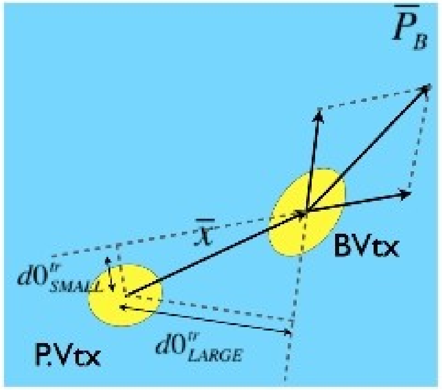

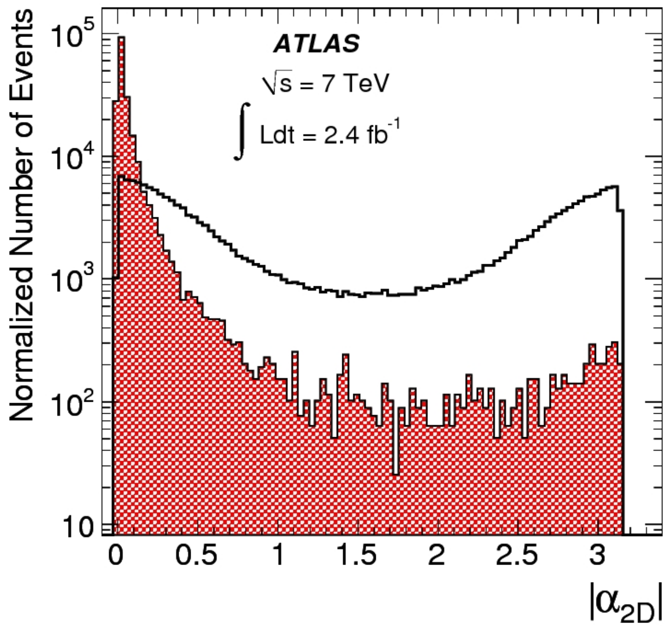

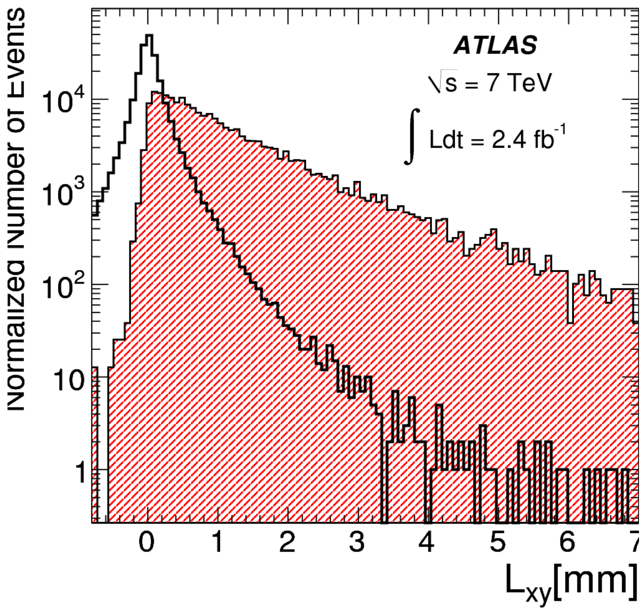

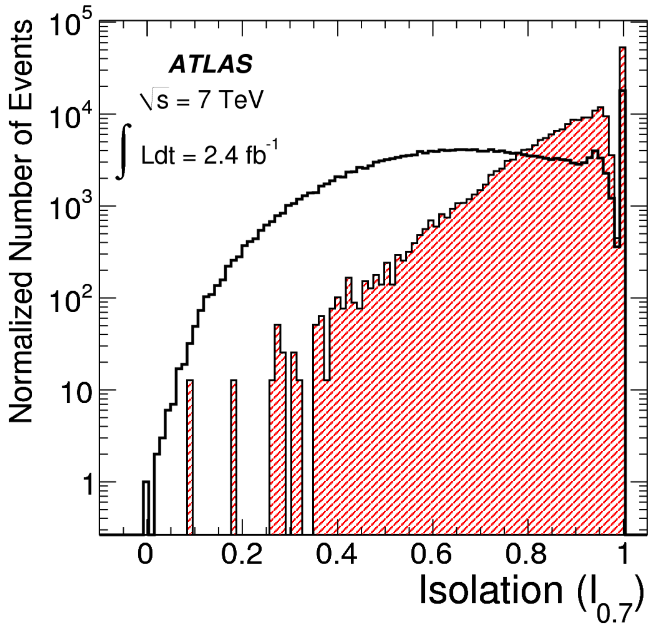

isolation and pile-up

- Isolation variable:

$$I^{\Delta R} = \frac{P_T^B}{P_T^B + \sum_i^{\Delta R} p_T^i}$$

tracks with $p_T > 0.5$ GeV excluding B daughters in the cone $\Delta R < 0.7$, where $\Delta R = \mathrm{sqrt}((\Delta\eta)^2+(\Delta\phi)^2)$

- Solution: PV association of tracks:
  - gets rid of the interference from the other interactions
  - isolation cut efficiency is now pile-up independent

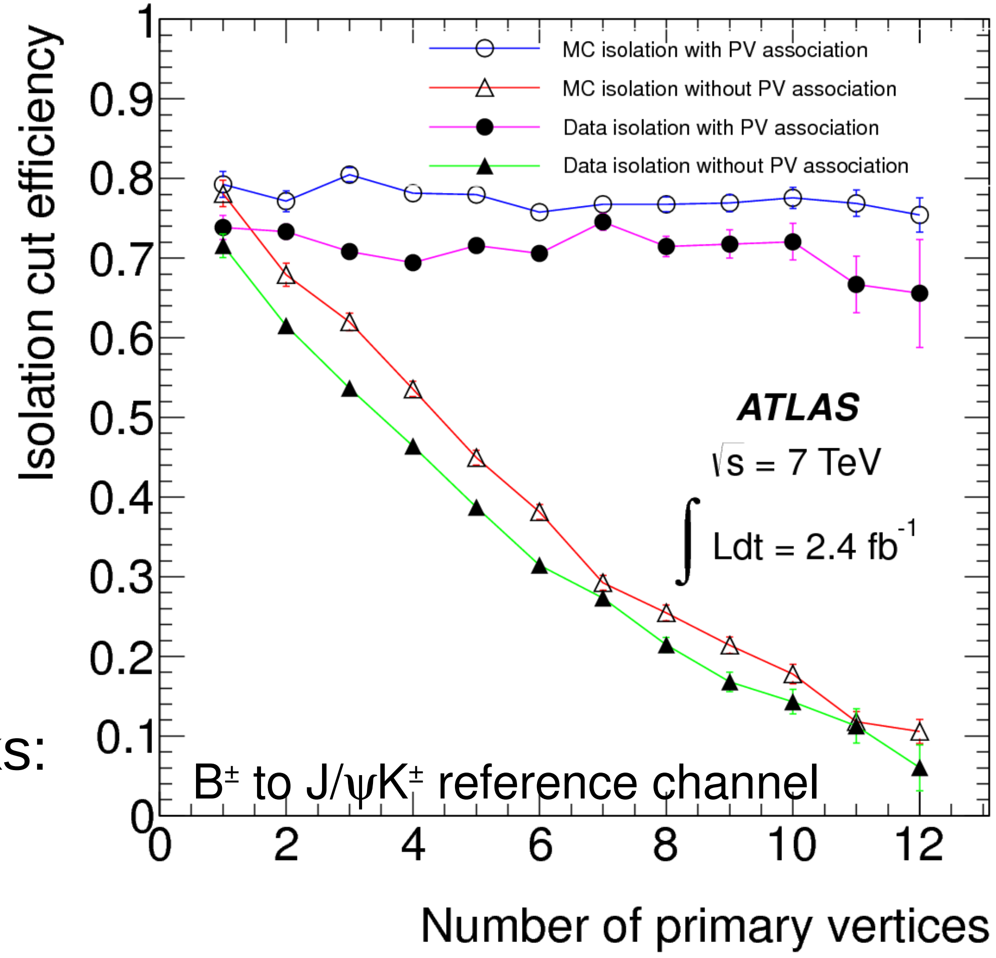

Boosted Decision Tree (BDT)

- Multivariate techniques used to combine the separation power of the 14 discriminating variables chosen.

- Optimize estimator: $$\mathcal{P} = \frac{\epsilon_{\text{sig}}}{\frac{a}{2} + \sqrt{N_{\text{bkg}}}}$$

(a=2 for 95% CL limit)

- among the classifiers tested, BDT is the best performing
- trained using $B_s \to \mu^+\mu^-$ signal MC and data from sidebands (50% of the events)
- then BDT cut and mass search window optimized by maximizing the estimator above

Boosted Decision Tree (BDT)

- Multivariate techniques used to combine the separation power of the 14 discriminating variables chosen.

B_s signal (MC) vs **background (sidebands)**
⇒ clear separation

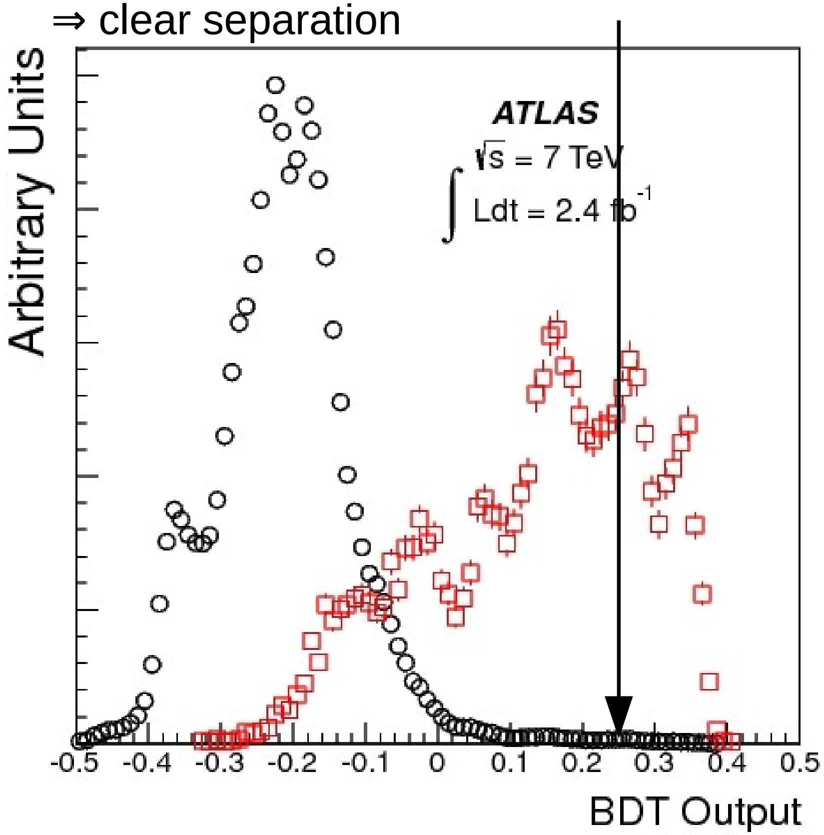

$B^{\pm}$ data (sideband subtracted)
vs **MC (weighted)** ⇒ good agreement

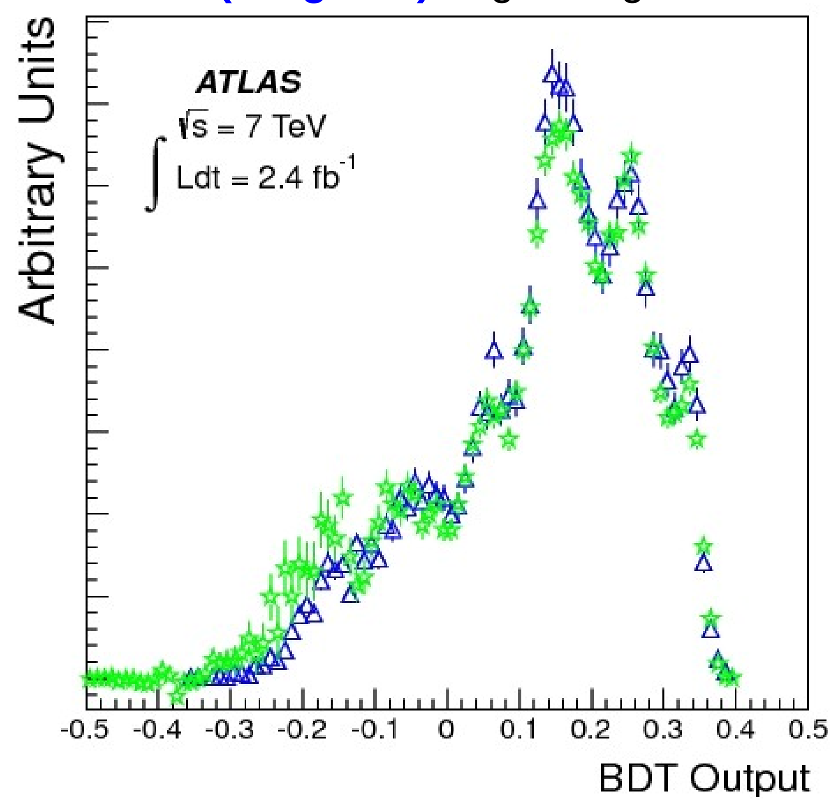

- optimal cut at ~0.25
- good S/B separation
- MC reproduces response on data pretty well!

mass resolution categories

- Three mass resolution categories are defined according to the η of the muons in the final state

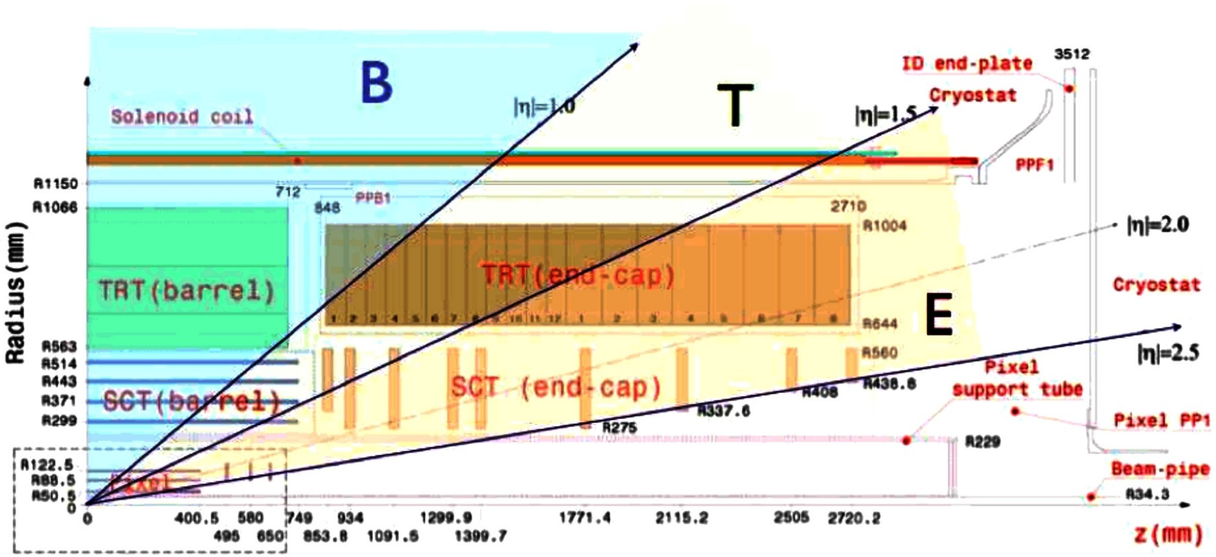

- Mass resolution for di-muon candidates changes substantially between barrel and end-cap detectors

$\|\eta_{max}\|$	1.0	1.5	2.5
σ_m [MeV]	60	80	110
Relative fraction [%]	51	24	25
invariant mass window [MeV]	±116	±133	±171
BDT output threshold	0.234	0.245	0.270

ingredient for the limit extraction

$|\eta|_{\max}$ Range	0–1.0	1.0–1.5	1.5–2.5
$B^{\pm} \to J/\psi K^{\pm} \to \mu^+\mu^- K^{\pm}$	4300	1410	1130
statistical uncertainty	±1.6%	±2.8%	±3.0%
systematic uncertainty	±2.9%	±7.4%	±14.1%

$|\eta_{max}|$ Range	$R^i_{A\epsilon}$	Δ % Stat.	Δ % Syst.
0-1.0	0.274	3.1	3.1
1.0-1.5	0.202	4.8	5.5
1.5-2.5	0.143	5.3	5.9

$$BR(B_s \to \mu\mu) = N_{B_s\to\mu\mu} \frac{1}{N_{B^{\pm}\to J/\psi K^{\pm}}} BR(B^{\pm} \to J/\psi K^{\pm}) \frac{f_u}{f_s} \frac{\varepsilon_{B^{\pm}\to J/\psi K^{\pm}}}{\varepsilon_{B_s\to\mu\mu}} \frac{A_{B^{\pm}\to J/\psi K^{\pm}}}{A_{B_s\to\mu\mu}}$$

$1/(4.45\pm0.38)\times10^3$

[PDG + LHCb]

Additional sources of systematics:

- vertex reconstruction efficiency in data/MC
- absolute $K^{\pm}$ reconstruction efficiency
- asymmetry in detector response to K^+/K^-

ingredient for the limit extraction

$\lvert\eta\rvert_{\max}$ Range	0–1.0	1.0–1.5	1.5–2.5
$B^{\pm} \to J/\psi K^{\pm} \to \mu^+\mu^- K^{\pm}$	4300	1410	1130
statistical uncertainty	±1.6%	±2.8%	±3.0%
systematic uncertainty	±2.9%	±7.4%	±14.1%

$\lvert\eta_{max}\rvert$ Range	$R^{i}_{A\epsilon}$	Δ % Stat.	Δ % Syst.
0-1.0	0.274	3.1	3.1
1.0-1.5	0.202	4.8	5.5
1.5-2.5	0.143	5.3	5.9

$$BR(B_s \to \mu\mu) = N_{B_s\to\mu\mu} \frac{1}{N_{B^{\pm}\to J/\psi K^{\pm}}} \; BR(B^{\pm} \to J/\psi K^{\pm}) \frac{f_u}{f_s} \; \frac{\varepsilon_{B^{\pm}\to J/\psi K^{\pm}}}{\varepsilon_{B_s\to\mu\mu}} \frac{A_{B^{\pm}\to J/\psi K^{\pm}}}{A_{B_s\to\mu\mu}}$$

$1/(4.45\pm0.38)\times10^{3}$
[PDG + LHCb]

$\lvert\eta\rvert_{\max}$ Range	0–1.0	1.0–1.5	1.5–2.5
SES= $(\epsilon\epsilon_i)^{-1}$ $[10^{-8}]$	0.71	1.6	1.4

reference channel yield

- keep selection as close to Bs as possible
- BDT trained for B_s used also on B^+, in order to minimize selection systematics
- inclusion of per-event mass resolution in the fit
- Systematic uncertainties on the yield
  - Vary binning
  - Signal/background models
  - Binned/un-binned fit

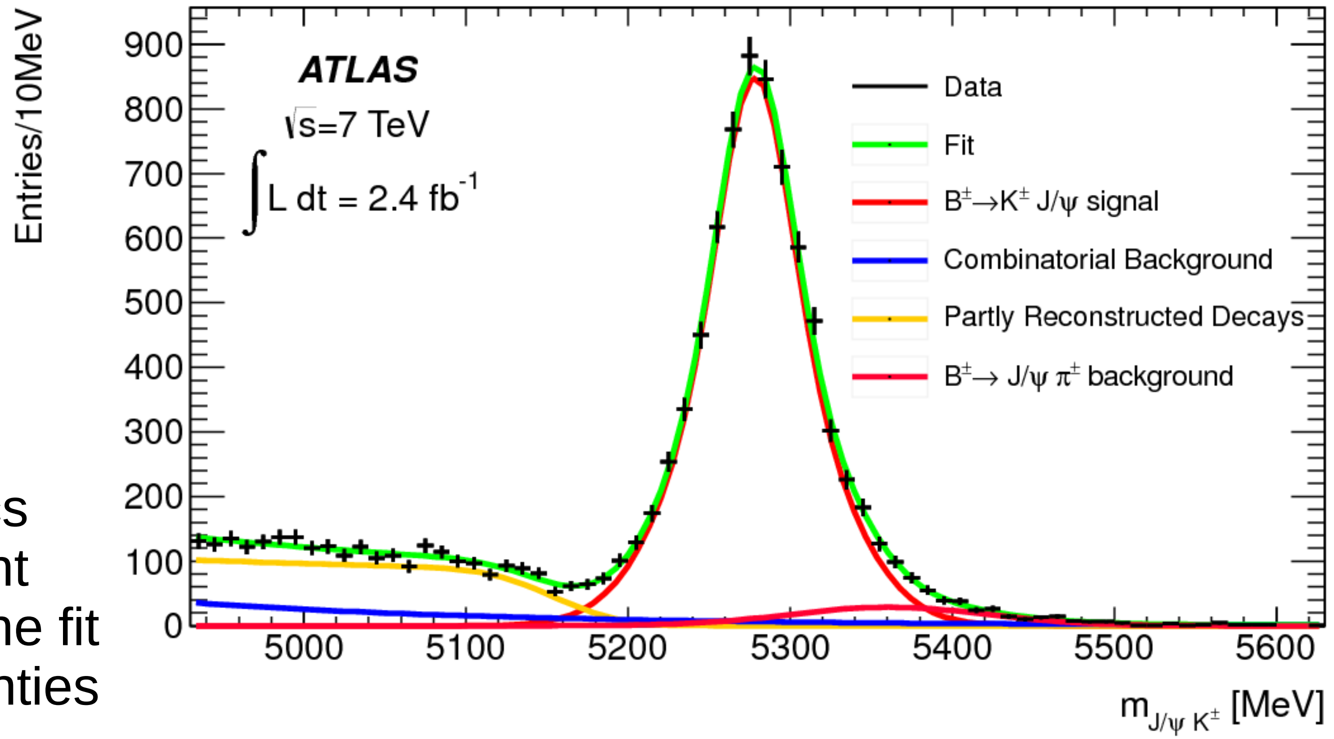

$B^\pm$ yield measurement only on even-numbered events
odd-numbered events used for MC re-weighting

$\|\eta\|_{\max}$ Range	0–1.0	1.0–1.5	1.5–2.5
$B^\pm \to J/\psi K^\pm \to \mu^+\mu^- K^\pm$	4300	1410	1130
statistical uncertainty	±1.6%	±2.8%	±3.0%
systematic uncertainty	±2.9%	±7.4%	±14.1%

opening the box

60 MeV resolution

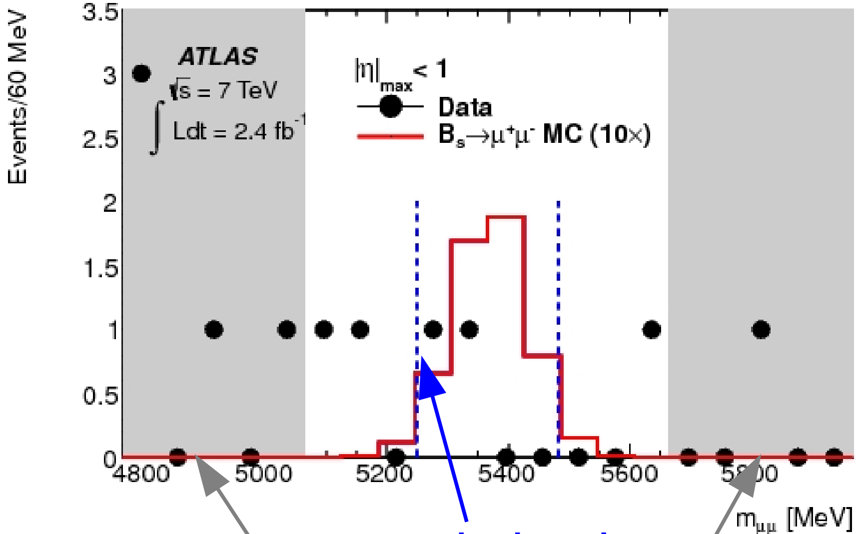

optimized search window

sidebands

80 MeV resolution

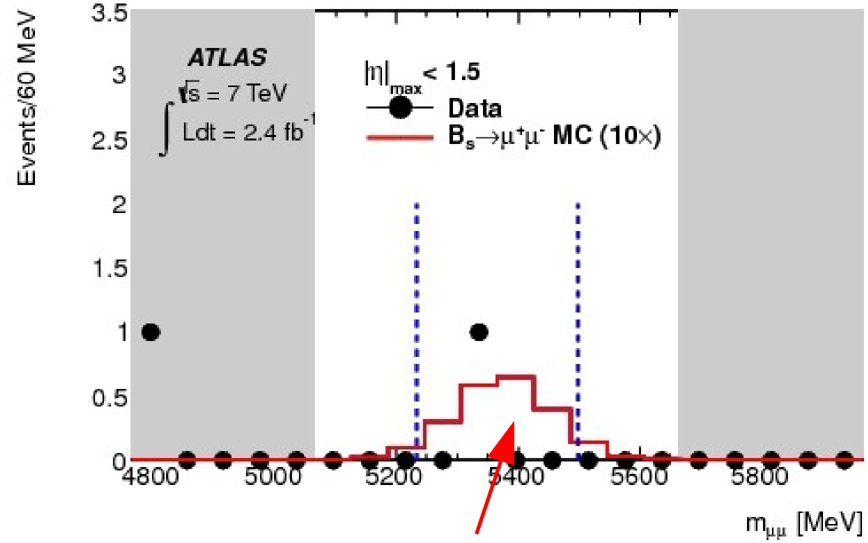

signal peak 10 times enhanced

110 MeV resolution

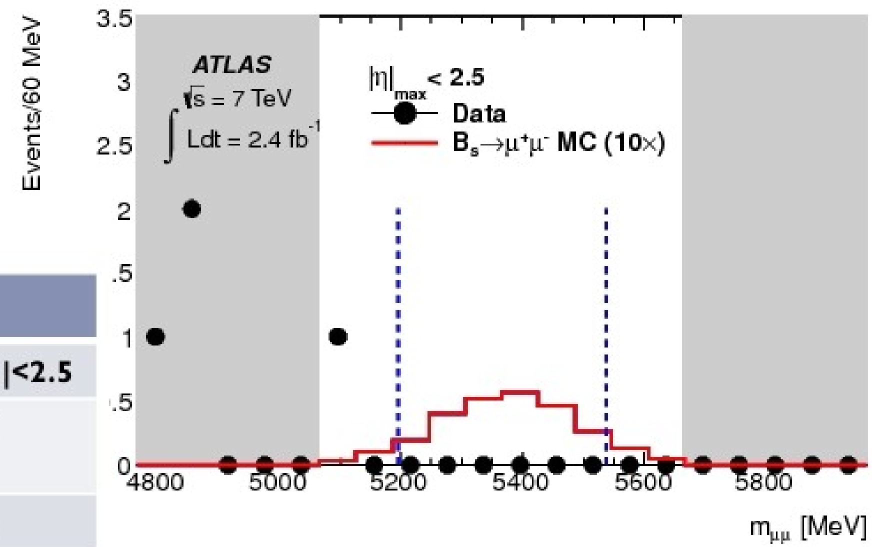

	Mass Resolution bins		
	$|\eta|<1.0$	$1.0<|\eta|<1.5$	$1.5<|\eta|<2.5$
Events in sidebands (unbiassed)	5	0	2
Events in sidebands (biassed)	1	1	1
Expected bkg event in SR	3.86	0	2.28
Expected resonant bkg	0.1	0.06	0.8
Observed events in SR	2	1	0

angular analysis in $B_s \to J/\psi\phi$

In the decay $\overline{B}_S(B_S) \to J/\psi\phi \to l^+l^- K^+K^-$
different components in the angular-distributions amplitudes correspond to CP = +1 or -1.
The "transversity angles" are used to describe the angular distributions:

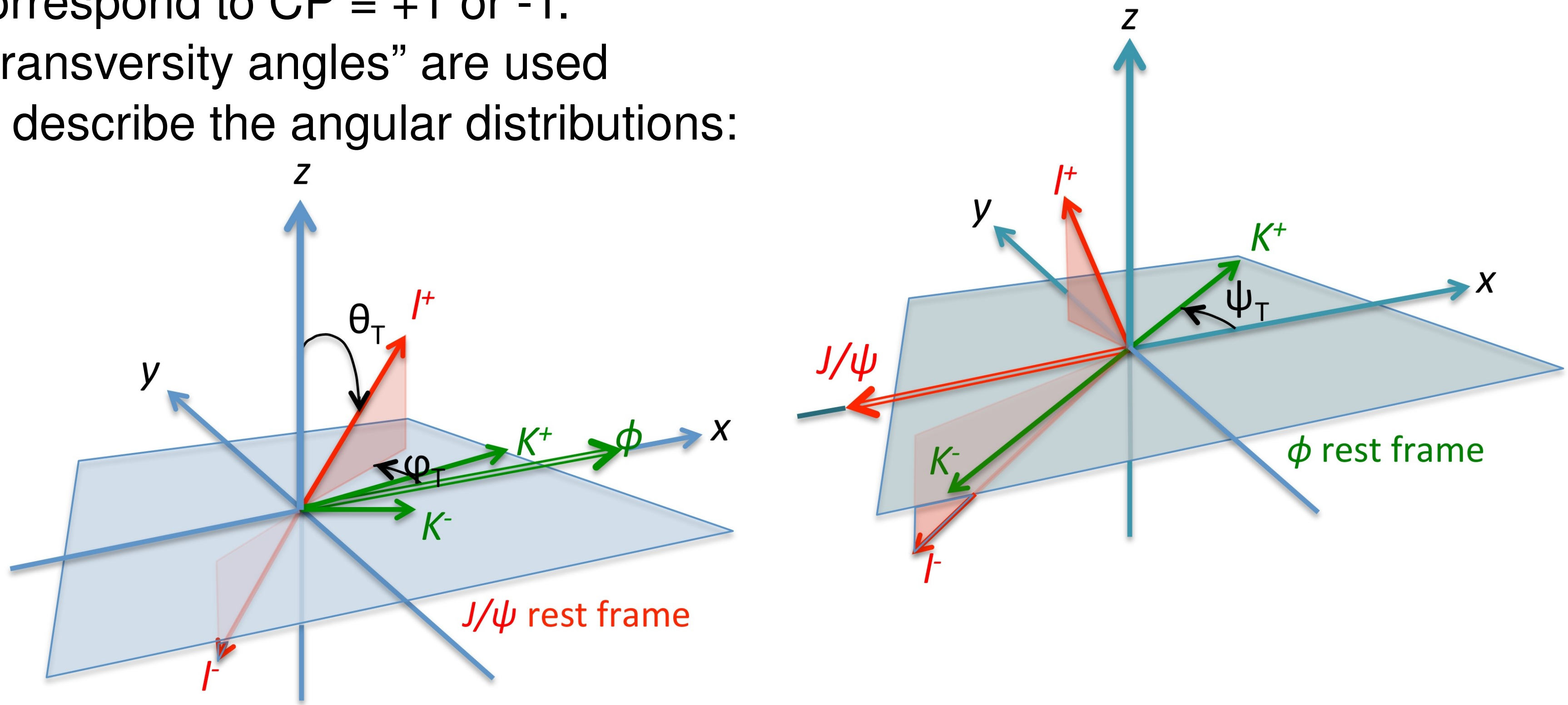

In the J/ψ (or ϕ) rest frames, the direction of ϕ (opposite to J/ψ) defines the x axis, and the xy-plane is defined by the K^+K^- decay plane, with K^+ oriented towards positive y; θ_T and φ_T are the polar angles of l^+, ψ_T is the angle between K^+ and x-axis

the measurement of ATLAS in $B_s \to J/\psi\phi$

Analysis using data collected in 2011 (4.7 fb^{-1}).
Trigger selection based in di-muon and single-muon triggers
 (p_T threshold 4 GeV or higher)
Offline selection based on J/ψ and ϕ invariant masses, χ^2/NDF< 3
 in fit to decay vertex, $|\eta|<2.5$ for all tracks,
 $p_T > 0.5$ GeV for kaon candidates.
Decay time computed in the plane normal to collision axis.
Average number of primary interactions 5.6:
 wrong association to primary vertex is < 1% and
 effects are negligible.
Acceptance computed on large samples of signal and background channels
 (e.g.: $B^0 \to J/\psi K^{*0}$, bb $\to J/\psi$ X, pp $\to J/\psi$ X).
Efficiency via data-driven procedures.

maximum likelihood fit

$$\ln\ \mathcal{L} = \sum_{i=1}^{N} \{ w_i \cdot \ln(f_s \cdot \mathcal{F}_s(m_i, t_i, \Omega_i) + f_s \cdot f_{B^0} \cdot \mathcal{F}_{B^0}(m_i, t_i, \Omega_i) + (1 - f_s \cdot (1 + f_{B^0}))\mathcal{F}_{bkg}(m_i, t_i, \Omega_i))\} + \ln P(\delta_\perp)$$

the signal with relative amplitude described by the parameter f_s.

the background due to $B^0 \to J/\psi K^{*0}$ and $B^0 \to J/\psi K\pi$ (non resonant), described by the parameter f_{B^0}, constrained by known branching fractions and acceptance (11% of signal amplitude)

the prompt and non-prompt combinatorial background described with empirical angular distribution. (No K-π discrimination.)
w_i describes a small trigger inefficiency (~1%)..

systematic uncertainties

Systematic	ϕ_s(rad)	$\Delta\Gamma_s$(ps^{-1})	Γ_s(ps^{-1})	$\lvert A_{\parallel}(0)\rvert^2$	$\lvert A_0(0)\rvert^2$	$\lvert A_S(0)\rvert^2$
Inner Detector alignment	0.04	< 0.001	0.001	< 0.001	< 0.001	< 0.01
Trigger efficiency	< 0.01	< 0.001	0.002	< 0.001	< 0.001	< 0.01
Signal mass model	0.02	0.002	< 0.001	< 0.001	< 0.001	< 0.01
Background mass model	0.03	0.001	< 0.001	0.001	< 0.001	< 0.01
Resolution model	0.05	< 0.001	0.001	< 0.001	< 0.001	< 0.01
Background lifetime model	0.02	0.002	< 0.001	< 0.001	< 0.001	< 0.01
Background angles model	0.05	0.007	0.003	0.007	0.008	0.02
B^0 contribution	0.05	< 0.001	< 0.001	< 0.001	0.005	< 0.01
Totals	0.10	0.008	0.004	0.007	0.009	0.02

These are calculated with different techniques, including:

- changes in detector simulation (alignment),
- data based studies (efficiency),
- pseudo-experiments Montecarlo (mass models, background angles)
- and variations in analysis methods and assumptions.

symmetries in the likelihood of $B_s \to J/\psi\phi$ analysis

The term describing $B_S \to J/\psi\ \phi$ in the likelihood is invariant under the transformations:

$$\{\phi_s, \Delta\Gamma_s, \delta_\perp, \delta_\parallel\} \to \{\pi - \phi_s, -\Delta\Gamma_s, \pi - \delta_\perp, 2\pi - \delta_\parallel\}$$

$$\{\phi_s, \Delta\Gamma_s, \delta_\perp, \delta_\parallel\} \to \{-\phi_s, \Delta\Gamma_s, \pi - \delta_\perp, 2\pi - \delta_\parallel\}$$

with the latter characteristic of untagged analyses.

The ATLAS analysis favours values of ϕ_S close to 0 (π),
for which an untagged analysis is scarcely sensitive to the phase $\delta_\perp$.

We therefore proceed as follows:

we constrain the value of $\delta_\perp$ to 2.95 ± 0.39 rad
as recently measured (LHCb) [or its complement to π].

the four minima of the likelihood do not overlap, only one of them
is compatible with previous measurements, and we show
the result for that minimum.

result for ϕ_s and $\Delta\Gamma_s$ in $B_s \to J/\psi\phi$

Result of likelihood fit

Parameter	Value	Statistical uncertainty	Systematic uncertainty
ϕ_s(rad)	0.22	0.41	0.10
$\Delta\Gamma_s$(ps^{-1})	0.053	0.021	0.008
Γ_s(ps^{-1})	0.677	0.007	0.004
$\lvert A_0(0)\rvert^2$	0.528	0.006	0.009
$\lvert A_\parallel(0)\rvert^2$	0.220	0.008	0.007
$\lvert A_S(0)\rvert^2$	0.02	0.02	0.02

Correla1on coefficients

	ϕ_s	$\Delta\Gamma_s$	Γ_s	$\lvert A_0(0)\rvert^2$	$\lvert A_\parallel(0)\rvert^2$	$\lvert A_S(0)\rvert^2$
ϕ_s	1.00	−0.13	0.38	−0.03	−0.04	0.02
$\Delta\Gamma_s$		1.00	−0.60	0.12	0.11	0.10
Γ_s			1.00	−0.06	−0.10	0.04
$\lvert A_0(0)\rvert^2$				1.00	−0.30	0.35
$\lvert A_\parallel(0)\rvert^2$					1.00	0.09
$\lvert A_S(0)\rvert^2$						1.00

Likelihood profiles in the $\phi_s - \Delta\Gamma_s$ plane

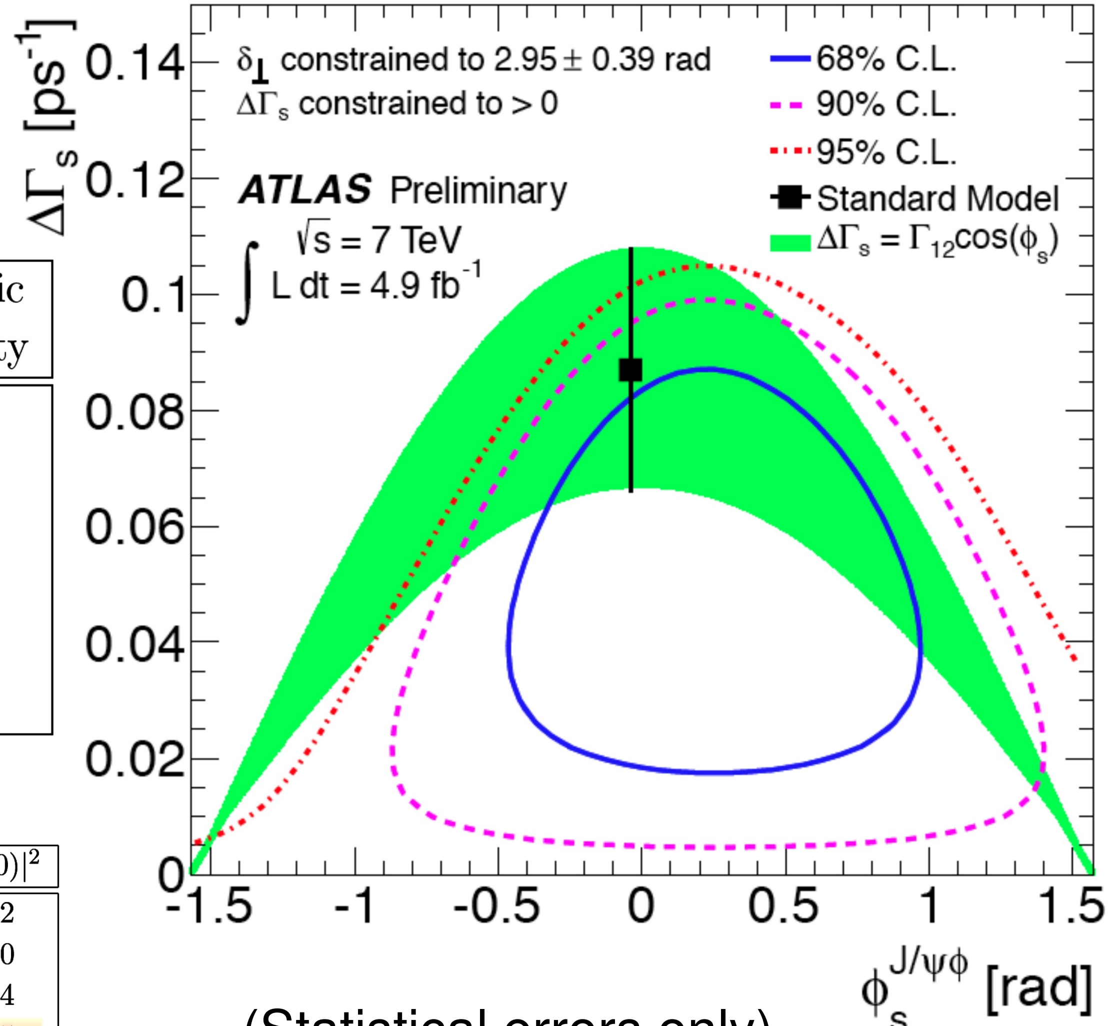

(Statistical errors only)
Agreement with the SM prediction